

TECHNICAL UNIVERSITY OF CRETE  
DEPARTMENT OF ELECTRICAL AND COMPUTERS ENGINEERS



# Development, technical and clinical validation of a multicolor pupillometric system

Anastasios Chatziioannou

Thesis Committee:

Professor Costas Balas

Associate Professor Aikaterini Mania

Associate Professor Aggelos Bletsas

*September 2018*

ΠΟΛΥΤΕΧΝΕΙΟ ΚΡΗΤΗΣ  
ΤΜΗΜΑ ΗΛΕΚΤΡΟΛΟΓΩΝ ΜΗΧΑΝΙΚΩΝ ΚΑΙ ΜΗΧΑΝΙΚΩΝ  
ΥΠΟΛΟΓΙΣΤΩΝ



Ανάπτυξη, τεχνική και κλινική αξιολόγηση  
συστήματος πολυχρωματικής κορημετρίας

Αναστάσιος Χατζιωάννου

Επιτροπή:

Καθηγητής Κώστας Μπάλας

Αναπληρώτρια Καθηγήτρια Μανιά Αικατερίνη

Αναπληρωτής Καθηγητής Μπλέτσας Άγγελος

*Σεπτέμβρης 2018*

## Table of Contents

Table of Figures .....	5
Abstract .....	7
Part 1: The human optical and nervous system .....	8
1.1 The human eye's anatomy.....	8
1.2 The human eye's pupil.....	9
1.3 Pupillary Light Reflex .....	10
1.4 Neural Pathways .....	11
1.4.1 The optic nerve .....	12
1.4.2 The oculomotor nerve.....	13
1.5 The Autonomic Nervous System.....	13
1.5.1 The Sympathetic Nervous System.....	14
1.5.2 The Parasympathetic Nervous System.....	15
Part 2: Pupillometry .....	16
2.1 Introduction to Pupillometry.....	16
2.2 Medical Uses .....	16
2.2.1 Chromatic Pupillometry.....	16
2.2.2 Eye nerve evaluation.....	17
2.2.3 Neurological Conditions .....	17
2.3 Cognitive Evaluation .....	17
2.3.1 Human Computer Interaction .....	17
2.3.2 Mind Wandering.....	18
2.3.4 Daytime Sleepiness .....	18
2.3.5 Depressive disorders.....	19
2.4 Pupillometry in Infancy .....	19
2.5 Substance consumption.....	19
2.6 Pupillometers .....	20
Part 3: Our custom pupillometer.....	22
3.1 List of Hardware Features.....	22
3.2 Components.....	22
3.2.1 Raspberry Pi Zero W .....	22
3.2.2 Raspberry Pi Zero .....	23

3.2.3 USB Connection .....	24
3.2.3 Raspberry Pi Camera .....	25
3.2.4 Optical Filters .....	26
3.2.5 Light diffuser .....	26
3.2.6 Light Emitting Diodes (LEDs) .....	27
3.2.7 Arduino Nano.....	42
3.2.8 LED Controller.....	43
3.2.9 Hull.....	43
3.3 Schematics .....	47
Part 4: Software .....	49
4.1 Graphical User Interface.....	49
4.1.1 Examinee’s profile .....	49
4.1.2 Lists of Patients and Examinations .....	50
4.1.3 Review Examination Menu .....	52
4.1.4 Recording a new examination (Scanner).....	55
4.2 Backend and Algorithms.....	56
4.2.1 Image Processing .....	56
4.2.2 Smoothing and Regression .....	61
4.2.3 Outlier Detection .....	62
4.2.4 Metrics Calculation .....	64
4.2.5 Technical Information.....	65
4.2.6 Database .....	66
4.2.7 Flowchart.....	67
Part 5: Measurements and results .....	69
5.1 Eye’s adaptability.....	70
5.2 Multicolor stimulation .....	71
References.....	73

## Table of Figures

Figure 1: The human eye.....	8
Figure 2: Phototransduction.....	9
Figure 3: The human eye's pupil.....	10
Figure 4: The neural pathways near the eye.....	11
Figure 5: The Autonomic Nervous System (ANS).....	14
Figure 6 : DIGITAL PUPILLOMETER / HAND-HELD PD-82 II.....	20
Figure 7: PC-based Desktop Pupillometer with 4-color stimulus.....	21
Figure 8: Raspberry Pi Zero W.....	23
Figure 9: Raspberry Pi Zero.....	24
Figure 10: USB Mini-B to USB Mini B cable.....	24
Figure 11: Raspberry Pi Camera.....	25
Figure 12: Light diffuser and Optical filter.....	26
Figure 13: Androgenic effects on PLR.....	27
Figure 14: 430nm LED full spectrum. (Intensity vs wavelength in nm).....	28
Figure 15: 430nm LED.....	28
Figure 16: 460nm LED full spectrum. (Intensity vs wavelength in nm).....	29
Figure 17: 460nm LED.....	29
Figure 18: 470nm LED full spectrum. (Intensity vs wavelength in nm).....	30
Figure 19: 470nm LED.....	30
Figure 20: 515nm Full Spectrum (Intensity vs wavelength in nm).....	31
Figure 21: 515nm LED.....	31
Figure 22: 535nm LED spectrum (Intensity vs wavelength in nm).....	32
Figure 23: 535nm LED.....	32
Figure 24: 569nm LED spectrum (Intensity vs wavelength in nm).....	33
Figure 25: 569nm LED.....	33
Figure 26: 587nm LED spectrum (Intensity vs wavelength in nm).....	34
Figure 27: 587nm LED.....	34
Figure 28: 605nm LED Full Spectrum (Intensity vs wavelength in nm).....	35
Figure 29: 605nm LED.....	35
Figure 30: 645nm LED Full Spectrum (Intensity vs wavelength in nm).....	36
Figure 31: 645nm LED.....	36
Figure 32: 700nm LED Full Spectrum (Intensity vs wavelength in nm).....	37
Figure 33: 700nm LED.....	37
Figure 34: 730nm LED Full Spectrum (Intensity vs wavelength in nm).....	38
Figure 35: 730nm LED.....	38
Figure 36: Monochromatic LED spectra (Intensity vs wavelength in nm).....	39
Figure 37: Cold White LED Full Spectrum.....	39
Figure 38: Warm White LED Full Spectrum.....	40
Figure 39: Final (True White) white LED combination.....	40
Figure 40: White LED.....	41
Figure 41: Infrared LEDs.....	41

Figure 42: Arduino Nano.....	42
Figure 43: TLC 5940.....	43
Figure 44: The shell of the device .....	44
Figure 45: Light eliminating cloth.....	44
Figure 46: Inside the device.....	45
Figure 47: Top View of the Device.....	46
Figure 48: Rear View of the Device .....	46
Figure 49: Motherboard Schematics [Low Level].....	47
Figure 50: Motherboard Schematics [Top Level].....	47
Figure 51: Hardware Flowchart .....	48
Figure 52: Examinee's profile.....	50
Figure 53: List of patients .....	51
Figure 54: List of exams.....	51
Figure 55: Past Examination Overview .....	52
Figure 56: Diameter vs Time, Green Stimulus .....	54
Figure 57: Diameter vs Time, Multiple Stimuli .....	54
Figure 58: Find max serial black pixels .....	57
Figure 59: Find three contour points .....	57
Figure 60: Algorithm's output.....	58
Figure 61: Original Image .....	58
Figure 62: Thresholding the image.....	59
Figure 63: Blurring the thresholded image.....	59
Figure 64 : Canny Edge Detector .....	60
Figure 65: Final output of the image processing.....	60
Figure 66: Graphs before smoothing (Left - Right) .....	61
Figure 67: Graphs after smoothing (Left - Right).....	61
Figure 68: Blinking spikes .....	62
Figure 69: Outlier Detection .....	63
Figure 70: Graphical User Interface Flowchart.....	67
Figure 71: Software Flowchart.....	68
Figure 72: Reviewing Examinations.....	69
Figure 73: Examination patterns.....	70
Figure 74: Slow accommodation to light.....	70
Figure 75: Homeostatic imbalance .....	71
Figure 76: Graph drawing timelines.....	71
Figure 77: Multicolor Overlapping.....	72
Figure 78: Multicolor Overlapping Extended.....	72

## Abstract

The pupil is a small black hole in the middle of the eye and the iris is the colored part. When light is shone upon the eye, the iris constricts, reducing the pupil in size, in order to calibrate the brightness inside the eye. Respectively, when no light is present, the pupil dilates. This phenomenon is called Pupillary Light Reflex. The pupillary reflex is controlled by the Autonomous Nervous System (ANS). Consequently, any extraordinary behavior during measurement may indicate underlying neurological problems. Pupillometry is the study of recording the changes of the pupil's diameter, using a light stimulus. Scientific research has shown that pupillometry can be used to detect some neurological and psychological conditions. Pupillometry may also be used as a detection tool for illicit substance use. For the purposes of this project, a custom pupillometric device was created from scratch, along with the software that interacts with it. The Graphical User Interface provides all the necessary details that the examiner should require during an examination. All the results are calculated by the software, using algorithms created specifically for this project. Most pupillometric projects prefer white color LEDs that cover most of the visible spectrum. In this project we will extend our focus to multicolor (monochromatic) stimuli, in order to record and report any sensitivity to specific wavelengths. This pupillometric device is a very powerful tool in the hands of neurosurgeons, anesthesiologists, as well as psychiatrists.

## Part 1: The human optical and nervous system

### 1.1 The human eye's anatomy

The human eyes are the organs responsible for reacting to light and colors and forming images that are then interpreted by the brain. The biology of the eye permits light to enter through the pupil and be bent by a number of biological structures which are used to focus light onto the retina.

The eye is unique due to the result of what occurs when it reacts to light and pressure. The various structures of the eye work cooperatively to accept incoming light rays in order to focus an image onto the retina. The human eye is comprised of many components as is seen in the diagram below:

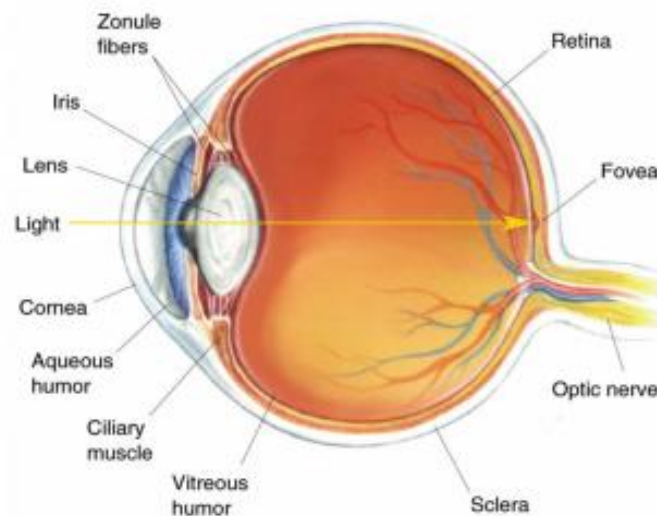


Figure 1: The human eye.

The light rays entering the eye first encounters the cornea which is the transparent layer covering the pupil. The opening to the inner eye is called the pupil and this is responsible for controlling the amount of light entering the eye. The iris (ring shaped membrane surrounding the eye composed of muscle fibers) does this by constricting or dilating the pupil.

Once past the pupil, the light rays entering the inner eye are bent by the crystalline lens. The lens is an instrumental tool which works cooperatively with the cornea to bend and focus light. In order to accommodate for different object distances, the lens is able to change shape, via the action of the ciliary muscle in order to change the focal point of the lens, which is the point at which all of the light rays collect. Ideally the light rays would collect on the inner wall of the eye known as the retina on a point called the fovea. The Fovea are layers of the retina, which are spread aside to let light fall directly on the sensory cells. This area contains the cone and rod photoreceptors which are used to perceive light and color and converts the light into electrical impulses. Of particular importance on this bed of photoreceptors is the optic disk, or the region of the fovea where the nerve bundles for the optic nerve are gathered, connecting this to the retina, and rendering this a blind spot on the retina – as well

as the converse of this, the fovea centralis. The latter serves as the point on the retina where images are processed to the highest acuity, and is in close proximity to the optic disk.

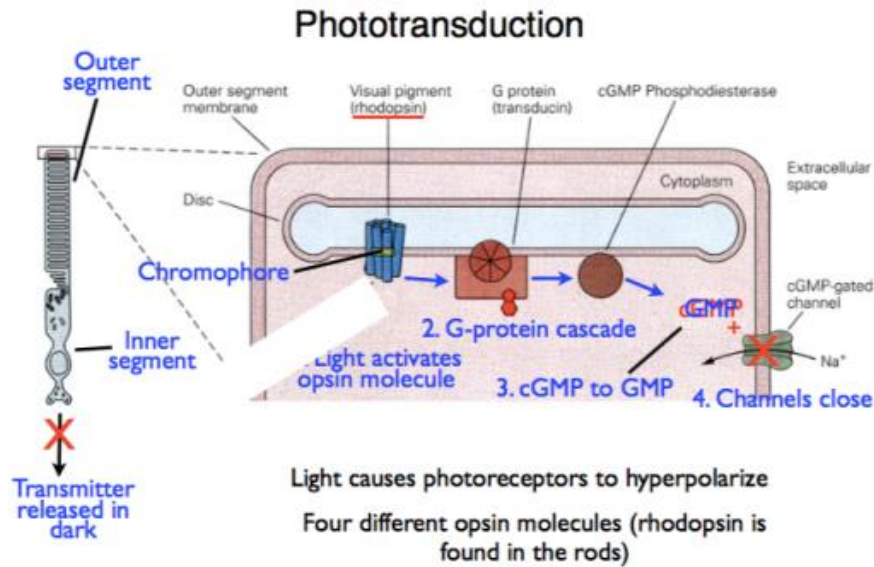


Figure 2: Phototransduction.

A brief outline of phototransduction offers a glimpse into the biochemical processes at play – within a rod cell, for example, which is responsible for sight at nighttime, and in low light conditions, there is a single opsin molecule (visual pigment) called rhodopsin that is manifested in billions of tiny stacked structures that are highly sensitive to faint light. Normally in rods, the membrane is depolarized as the sodium channels are open to allow influx of  $\text{Na}^+$  ions into the cytoplasm, and neurotransmitter release. However, once chromophores become active, as during light exposure, rhodopsin triggers a G-protein cascade that converts cGMP to GMP in the rod cytoplasm, resulting in cessation of  $\text{Na}^+$  ions coming in by opening of  $\text{Na}^+$  ion channels and hyperpolarization of the cell. This is what occurs in cones, which also contain 3 chromatic opsins that enable us to distinguish the colors around us. Once the information has been converged onto the middle layer of the retina, bipolar and amacrine cells are activated by the inverse process – a decrease in release of neurotransmitter from the first layer is responsible for their functioning.

## 1.2 The human eye's pupil

The pupil is a hole located in the center of the iris of the eye that allows light to strike the retina. It appears black because light rays entering the pupil are either absorbed by the tissues inside the eye directly, or absorbed after diffuse reflections within the eye that mostly miss exiting the narrow pupil.

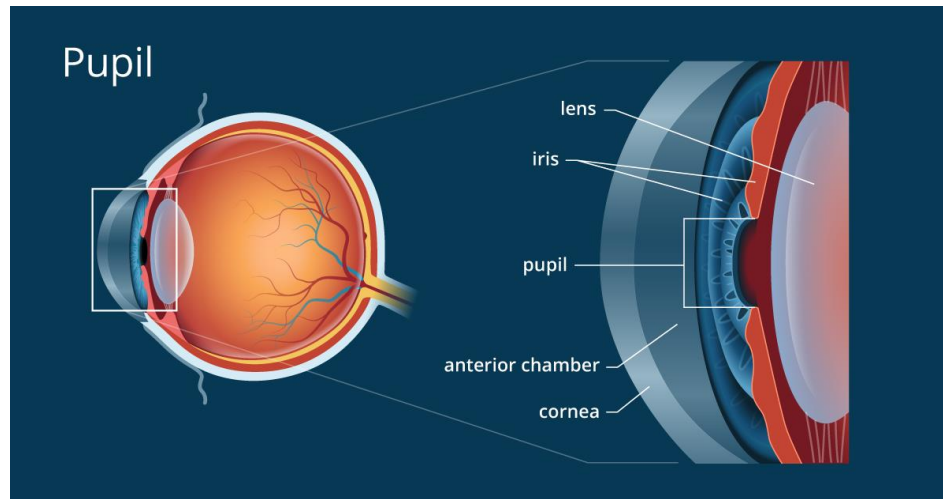


Figure 3: The human eye's pupil.

In optical terms, the anatomical pupil is the eye's aperture and the iris is the aperture stop. Based on analogy with a camera, pupil is equivalent to aperture, whereas iris is equivalent to the shutter. The image of the pupil as seen from outside the eye is the entrance pupil, which does not exactly correspond to the location and size of the physical pupil because it is magnified by the cornea. On the inner edge lies a prominent structure, the collarette, marking the junction of the embryonic pupillary membrane covering the embryonic pupil.

### 1.3 Pupillary Light Reflex

The pupillary light reflex (PLR) or photopupillary reflex is a reflex that controls the diameter of the pupil, in response to the intensity (luminance) of light that falls on the retinal ganglion cells of the retina in the back of the eye, thereby assisting in adaptation to various levels of lightness/darkness. A greater intensity of light causes the pupil to constrict (miosis/myosis; thereby allowing less light in), whereas a lower intensity of light causes the pupil to dilate (mydriasis, expansion; thereby allowing more light in). Thus, the pupillary light reflex regulates the intensity of light entering the eye.

Light shone into one eye will cause both pupils to constrict. A direct pupillary reflex is pupillary response to light that enters the ipsilateral (same) eye. A consensual pupillary reflex is response of a pupil to light that enters the contralateral (opposite) eye. Thus there are four types of pupillary light reflexes, based on this terminology of absolute (left versus right) and relative (same side versus opposite side) laterality:

- i. Left direct pupillary reflex is the left pupil's response to light entering the left eye.
- ii. Left consensual pupillary reflex is the left pupil's indirect response to light entering the right eye, the contralateral eye.
- iii. Right direct pupillary reflex is the right pupil's response to light entering the right eye.
- iv. Right consensual pupillary reflex is the right pupil's indirect response to light entering the left eye, the contralateral eye.

## 1.4 Neural Pathways

The pupillary light reflex neural pathway on each side has an *afferent* limb and two *efferent* limbs.

**Afferent neurons** are sensory neurons that carry nerve impulses from sensory stimuli towards the central nervous system and brain, while **efferent neurons** are motor neurons that carry neural impulses away from the central nervous system and towards muscles to cause movement.

The afferent limb has nerve fibers running within the optic nerve (CN II). Each efferent limb has nerve fibers running along the oculomotor nerve (CN III). The afferent limb carries sensory input. Anatomically, the afferent limb consists of the retina, the optic nerve, and the pretectal nucleus in the midbrain, at level of superior colliculus. Ganglion cells of the retina project fibers through the optic nerve to the ipsilateral pretectal nucleus.

The efferent limb is the pupillary motor output from the pretectal nucleus to the ciliary sphincter muscle of the iris. The pretectal nucleus projects crossed and uncrossed fibers to the ipsilateral and contralateral Edinger-Westphal nuclei, which are also located in the midbrain. Each Edinger-Westphal nucleus gives rise to preganglionic parasympathetic fibers which exit with CN III and synapse with postganglionic parasympathetic neurons in the ciliary ganglion. Postganglionic nerve fibers leave the ciliary ganglion to innervate the ciliary sphincter.

Each afferent limb has two efferent limbs, one ipsilateral and one contralateral. The ipsilateral efferent limb transmits nerve signals for direct light reflex of the ipsilateral pupil. The contralateral efferent limb causes consensual light reflex of the contralateral pupil.

The **optic nerve**, or more precisely, the photosensitive ganglion cells through the retinohypothalamic tract, is responsible for the *afferent* limb of the pupillary reflex; it senses the incoming light. The **oculomotor nerve** is responsible for the *efferent* limb of the pupillary reflex; it drives the iris muscles that constrict the pupil.

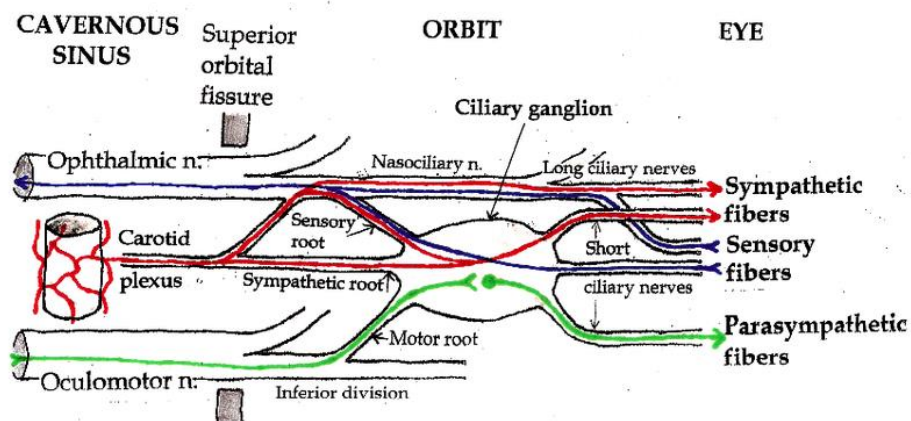


Figure 4: The neural pathways near the eye.

### 1.4.1 The optic nerve

The optic nerve transmits all visual information including brightness perception, color perception and contrast (visual acuity). It also conducts the visual impulses that are responsible for two important neurological reflexes: the light reflex and the accommodation reflex. The light reflex refers to the constriction of both pupils that occurs when light is shone into either eye; the accommodation reflex refers to the swelling of the lens of eye that occurs when one looks at a near object as in reading (lens adjusts to near vision).

The eye's blind spot is a result of the absence of photoreceptors in the area of the retina where the optic nerve leaves the eye.

By far, the three most common injuries to the optic nerve are from glaucoma, optic neuritis (especially in those younger than 50 years of age), and anterior ischemic optic neuropathy (usually in those older than 50).

Causes of optic nerve injury:

- Glaucoma is a group of diseases involving loss of retinal ganglion cells causing optic neuropathy in a pattern of peripheral vision loss, initially sparing central vision. Glaucoma is associated with increased intraocular pressure that damages the optic nerve as it exits the eyeball. Although glaucoma does eventually damage the optic nerve, it is primarily a disease of eye not of the nerve.
- Optic neuritis is inflammation of the optic nerve. It is associated with a number of diseases, the most notable one being multiple sclerosis. The patient will likely experience varying vision loss and eye pain. The condition tends to be episodic.
- Anterior ischemic optic neuropathy is commonly known as "stroke of the optic nerve" and affects the optic nerve head. There is usually a sudden loss of blood supply and nutrients to the optic nerve head (where the nerve exits the eyeball). Vision loss is typically sudden and most commonly occurs upon waking up in the morning. This condition is most common in diabetic patients 40–70 years old.
- Optic nerve hypoplasia is the underdevelopment of the optic nerve resulting in little to no vision in the affected eye.
- Tumors, especially those of the pituitary gland, can put pressure on the optic nerve causing various forms of visual loss. Similarly, cerebral aneurysms (swelling of blood vessels) can also affect the nerve.
- Trauma can cause serious injury to the nerve. Direct optic nerve injury can occur from a penetrating injury to the orbit, but the nerve can also be injured by indirect trauma in which severe head impact or movement stretches or even tears the nerve.

### 1.4.2 The oculomotor nerve

The oculomotor nerve, besides enabling most movements of the eye and raising the eyelid, also controls the constriction of the pupils and thickening of the lens of the eye.

The oculomotor nerve can be examined through the pupillary light reflex.

Causes of oculomotor nerve malfunction:

- direct trauma
- demyelinating diseases (e.g., multiple sclerosis)
- increased intracranial pressure (leading to uncal herniation)
- due to a space-occupying lesion (e.g., brain cancer) or a
- spontaneous subarachnoid hemorrhage (e.g., berry aneurysm)
- microvascular disease, e.g., diabetes.

### 1.5 The Autonomic Nervous System

The autonomic nervous system (ANS), formerly the vegetative nervous system, is a division of the peripheral nervous system that supplies smooth muscle and glands, and thus influences the function of internal organs. The autonomic nervous system is a control system that acts largely unconsciously and regulates bodily functions such as:

- heart rate
- digestion
- respiratory rate
- **pupillary response**
- urination
- sexual arousal

The autonomic nervous system has two main branches: the *sympathetic* nervous system and the *parasympathetic* nervous system. The sympathetic nervous system is often considered the "fight or flight" system, while the parasympathetic nervous system is often considered the "rest and digest" or "feed and breed" system. In many cases, both of these systems have "opposite" actions where one system activates a physiological response and the other inhibits it. But this opposition is better termed complementary in nature rather than antagonistic. For an analogy, one may think of the sympathetic division as the accelerator and the parasympathetic division as the brake. The sympathetic division typically functions in actions requiring quick responses. The parasympathetic division functions with actions that do not require immediate reaction.

In general, these two systems should be seen as permanently modulating vital functions, in usually antagonistic fashion, to achieve homeostasis.

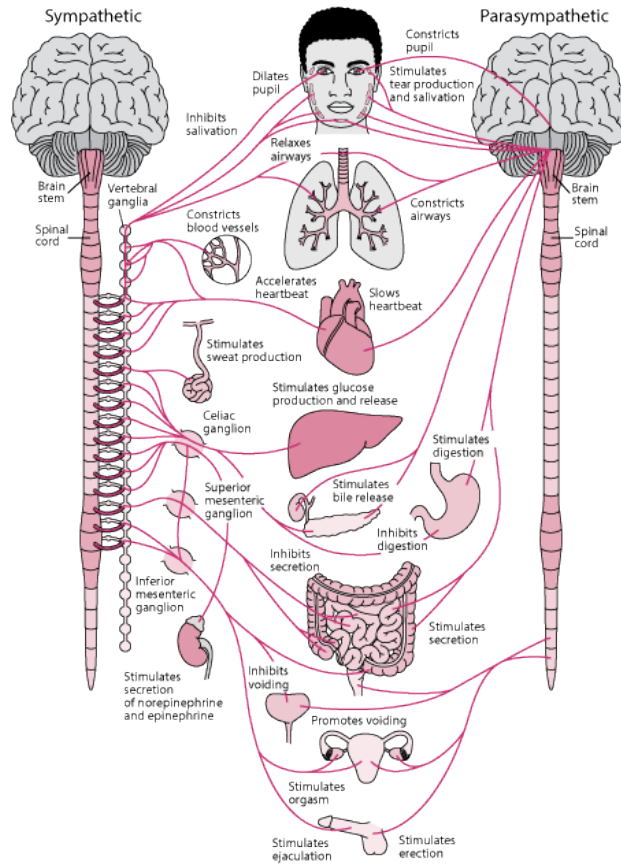


Figure 5: The Autonomic Nervous System (ANS)

### 1.5.1 The Sympathetic Nervous System

The autonomic nervous system functions to regulate the body's unconscious actions. The sympathetic nervous system's primary process is to stimulate the body's fight-or-flight response. It is, however, constantly active at a basic level to maintain homeostasis homeodynamics. The sympathetic nervous system is described as being complementary to the parasympathetic nervous system which stimulates the body to "feed and breed" and to (then) "rest-and-digest".

The sympathetic nervous system can control the below functions:

- Diverts blood flow away from the gastro-intestinal (GI) tract and skin via vasoconstriction
- Blood flow to skeletal muscles and the lungs is enhanced (by as much as 1200% in the case of skeletal muscles)
- Dilates bronchioles of the lung through circulating epinephrine, which allows for greater alveolar oxygen exchange
- Increases heart rate and the contractility of cardiac cells (myocytes), thereby providing a mechanism for enhanced blood flow to skeletal muscles
- **Dilates pupils** and relaxes the ciliary muscle to the lens, allowing more light to enter the eye and enhances far vision

- Provides vasodilation for the coronary vessels of the heart
- Constricts all the intestinal sphincters and the urinary sphincter
- Inhibits peristalsis
- Stimulates orgasm

### 1.5.2 The Parasympathetic Nervous System

The autonomic nervous system is responsible for regulating the body's unconscious actions. The parasympathetic system is responsible for stimulation of "rest-and-digest" or "feed and breed" activities that occur when the body is at rest, especially after eating, including sexual arousal, salivation, lacrimation (tears), urination, digestion and defecation. Its action is described as being complementary to that of the sympathetic nervous system, which is responsible for stimulating activities associated with the fight-or-flight response.

- Dilating blood vessels leading to the GI tract, increasing the blood flow.
- Constricting the bronchiolar diameter when the need for oxygen has diminished
- Dedicated cardiac branches of the vagus and thoracic spinal accessory nerves impart parasympathetic control of the heart (myocardium)
- **Constriction of the pupil** and contraction of the ciliary muscles, facilitating accommodation and allowing for closer vision
- Stimulating salivary gland secretion, and accelerates peristalsis, mediating digestion of food and, indirectly, the absorption of nutrients
- Sexual. Nerves of the peripheral nervous system are involved in the erection of genital tissues via the pelvic splanchnic nerves 2–4. They are also responsible for stimulating sexual arousal.

## Part 2: Pupillometry

### 2.1 Introduction to Pupillometry

Pupil size has been studied largely for its value as an indicator of cognitive workload, mental effort, attention, or affective processing. However, the pupil is usually studied under highly controlled conditions, as it is extremely sensitive to external factors such as changes in ambient light. In fact, the pupil dilation that occurs in response to a change in light exposure is much greater than that experienced as a result of cognitive processing. Additionally, pupil behavior is user- and session-dependent.

Almost a century after the first studies in this area, the field started to grow significantly (around the 1960s) and it piqued the interest of cognitive psychophysicists aiming at better understanding the functions of the brain and cognition. From the large body of research that then emerged, those cognitive states achieving the greatest acceptance as able to be inferred through pupil size are mental effort and cognitive overload. In a large set of studies, researchers have shown that there is a correlation between pupil size and the level of demands imposed by a cognitive task. That is, the more demanding the cognitive task, the greater the pupil size [Oswald Barral, 2016]. Today, clinicians routinely evaluate pupils as a component of the neurological examination and monitoring of critically ill patients, including patients with traumatic brain injury and stroke.

The most common pupillometric method exploits the Pupillary Light Reflex (PLR). By continuously measuring the pupil's size, once the eye is accustomed to the environment's current lighting condition (preferably a dark setting), an external light (stimulus) will be shone towards the eye for a short period of time – about 1 or 2 seconds. The pupil's measurement will stop once the pupil's size has reached its original resting size.

Once the examination procedure as described above is over, useful data and metrics can be extracted from the graph of Eye Diameter (pixels or mm) – Time (seconds).

### 2.2 Medical Uses

Pupillometry has multiple uses in contemporary medicine, and has been increasing in interest the past years. Measuring the eye's reactivity to light can help pinpoint problems regarding the eye's ability to perceive light and react to brightness changes. The Pupillary Light Reflex (PLR) is not only useful in monitoring how fast the eye can adapt to its surroundings, but there are also uses in diagnosing neurological diseases. The optical and oculomotor nerves, the ones responsible for perceiving light and reacting to changes, can be examined through the PLR. This concludes the statement that measuring the PLR may help one diagnose underlying neurological conditions, affecting the whole autonomic nervous system or strictly the nerves near the eye.

#### 2.2.1 Chromatic Pupillometry

Pupillometry using colored light stimulation has technologically advanced since the early experiments of the 60s and 70s. Chromatic pupillometry is now available as a small desktop or portable model.

The simplicity of the technique broadens the patient population to be tested and is thus well-suited for use in patients with limited mobility. However, testing protocols still tend to be longer than most typical clinical tests and the dark adaptation needed to improve rod sensitivity could be difficult in patients with limited comprehension or attention span, such as patients with cognitive decline and young children. Yet it is the pediatric population in whom chromatic pupillometry may be a potentially important tool to evaluate outer and inner retinal activity in a variety of retinal and neurologic disorders.

Portable chromatic pupillometry for children may be an alternative to electroretinography for assessing photoreceptor function. The distinct advantage of pupillometry is that electrodes are not necessary. One foreseeable application is the school vision screening test. The ease of portable pupillometry permits on-site testing of children who fail the screening test. Chromatic pupillometry may also be used to monitor children with retinal degenerative disorders. In patients with endstage photoreceptor degeneration, chromatic pupillometry has been shown to be more sensitive than full-field electroretinography in detecting residual levels of cone function. Conversely chromatic pupillometry has promise as a tool to detect recovery of photoreceptor function in children who undergo gene therapy who are still too young to provide reliable responses to subjective tests of vision. [3]

### 2.2.2 Eye nerve evaluation

Pupillometry can be a useful tool for detecting eye nerve malfunctions. Provided that low or non-existent light reactivity is detected, an ophthalmologist can diagnose an underlying condition. An exhaustive list of possible nerve conditions is discussed in 1.4.1, 1.4.2.

### 2.2.3 Neurological Conditions

Pupillometry may also be helpful in early detection of neurological diseases such as Alzheimer's, Parkinson's disease or ALS. Slow reactions to pupillary light stimulation may signal trouble in autonomic functions, affecting either the Sympathetic Nervous System (responsible for pupil dilation) or the Parasympathetic Nervous System (responsible for pupil constriction).

## 2.3 Cognitive Evaluation

### 2.3.1 Human Computer Interaction

Pupil size has been studied in cognitive sciences for more than a century and has been slowly introduced in the HCI field in the last few decades. Pupil size can be used to infer cognitive workload and mental effort in a reliable manner, and it also can be measured relatively inexpensively and unobtrusively. However, the extensive dependence on external factors such as ambient light conditions is slowing its progress beyond controlled laboratory experiments. In a promising development, recent research aimed at discriminating task-evoked pupillary responses from external-evoked pupillary responses has shown positive results, which augurs a productive future for

pupillometry in HCI. This may well herald application of the signal finding its way into less controlled set-ups ‘in the wild’. [Oswald Barral, 2016]

### 2.3.2 Mind Wandering

In our daily lives, we frequently find our attention drifting away from an ongoing task, focusing on unrelated private thoughts and feelings such as memories or prospective thoughts. In the majority of cases, this “shift in the focus of attention away from the here and now towards one’s private thoughts and feelings” (Smallwood, O’Connor, Sudbery, Obonsawin, 2007, p. 818) occurs spontaneously. We refer to this as mind wandering (MW; for a review: Smallwood & Schooler, 2015).

A significant body of literature has shown that the diameter of our eye pupils is affected by the cognitive and emotional demands of the task. For example, the pupils dilate in response to increased cognitive processing load (Hess & Polt, 1960; Kahneman & Beatty, 1966) and emotional load (Partala & Surakka, 2003). In addition, recent work has shown that the amplitude of pupillary response to light stimuli is indicative of the level of attention paid to those stimuli: the response is stronger when the light is attended (Binda & Murray, 2015; Binda, Pereverzeva, & Murray, 2013; Mathôt, van der Linden, Grainger, & Vitu, 2013; Naber, Alvarez, & Nakayama, 2013), indicating that pupil diameter is a rich source of information about the dynamics of cognition and perception. Hence, pupillometry can be a useful tool in understanding MW.

### 2.3.4 Daytime Sleepiness

Comprehensive clinical evaluation of excessive daytime sleepiness (EDS) includes diagnostic testing to distinguish narcolepsy, 20% of the sleep clinic population, from other primary sleep disorders (Partinen and Hublin, 2000). Multiple sleep latency test (MSLT), the de facto gold standard for objective measurement of sleepiness and differential diagnosis of narcolepsy has several limitations (Chervin et al., 1995; Johns, 2000; Littner et al., 2005), making it unreliable as the sole indicator of manifest sleepiness in narcolepsy (Kotterba et al., 2004; Wise, 2006).

Pupillometry is a brief, non-invasive, physiologically based technique shown to concur with behavioral indicators of sleepiness in several populations (Lichstein et al., 1994; Wilhelm et al., 1998a, 2001, 2009; Wilhelm, 2008), including in narcolepsy, where its use dates back several decades (Yoss et al., 1969, 1970). The interpretation of pupillometry-derived measures of sleepiness is limited by a lack of normative data and a robust “single-best” measure. Several pupillometry-derived measures of sleepiness, e.g., pupillary diameter and stability, pupillary light reflex have been examined in narcolepsy with discrepant results (Kollarits et al., 1982; Pressman et al., 1984; Norman and Dyer, 1987; O’Neill et al., 1996).

Pupillometry cannot substitute for the MSLT as a diagnostic tool in narcolepsy. However, given that the pupillometer is portable, the test protocol is short and the available metrics are reproducible without learning effects, tracking changes in PUI (or related indices) may prove to have value for longitudinal assessment in narcolepsy. It will be important for future studies to address the direct effects of modafinil and other approved drugs on pupillary dynamics and to directly examine longitudinal reliability and utility of these measures. [6]

### 2.3.5 Depressive disorders

Major depressive disorder is associated with abnormal autonomic regulation which could be noninvasively studied using pupillometry.

A study revealed diminished pupillary light reflex for left eye in girls suffering from major depression which could indicate abnormal depression-linked central parasympathetic control already in adolescent age. Additionally, the different results for left and right eye could be related to the effect of lateralization of cortical centers regulating autonomic nervous system.

### 2.4 Pupillometry in Infancy

The field of pupillometry in infancy and early childhood is relatively new. However, the wide array of applications of the measure ranging from physical cognition (Jackson & Sirois, 2009; Sirois & Jackson, 2012), social cognition (Gredebäck & Melinder, 2010, 2011; Hochmann & Papeo, 2014), emotion perception (Geangu, Hauf, Bhardwaj, & Bentz, 2011; Hepach & Westermann, 2013), motivation (Hepach, Vaish, & Tomasello, 2012, 2013), and application in clinical populations and their caregivers (e.g., Anderson, Colombo, & Shaddy, 2006; Falck-Ytter, 2008; Martineau, Hernandez, Hiebel, Roché, Metzger, & Bonnet-Brilhault, 2011) suggests a potential that is slowly but steadily emerging.

For infants and toddlers the world is more than a 'blooming and buzzing confusion' (Rakison & Oakes, 2008). Infants actively explore their environment to learn from both the physical and social world around them. In this sense (socio-) cognitive development is tied to the processing of novel information as concepts and representations are formed (Westermann, Mareschal, Johnson, Sirois, Spratling, & Thomas, 2007). Pupillometry offers a novel means to capture this processing. In contrast to looking time, pupil dilation does not suffer from a diminishing response over trials when participants become tired and less attentive because it does not require them to look at a stimulus for more than a few seconds (Jackson & Sirois, 2009; see also Sirois & Jackson, 2012, for a detailed discussion). Several studies have found measures of pupil dilation to be more sensitive to differences in experimental conditions than measures of looking time (Geangu et al., 2011; Jackson & Sirois 2009; Hepach & Westermann, 2013). In pupillometry, experimental designs are dynamic and pupillary changes can be assessed over brief time periods of time, too short to differentiate between experimental conditions with measures of looking times (Hepach & Westermann, 2013). [5]

### 2.5 Substance consumption

Pupillometry is becoming a relevant tool in Vision Sciences. So far, only a few studies have explored the relationship between pupil reflex measures and drug consumption. The aim of this study was to assess the applicability of dynamic mesopic pupillometry as an objective measurement method for the detection of blood alcohol levels above the legal limit. In a quasiexperimental design, 19 volunteers were asked to participate in two conditions (before and after alcohol intake). In session with alcohol intake, participants were asked to consume 27.5 ml of alcohol in 60 minute intervals for four hours. Pupillometry records were conducted by means of the Power Refractor II, using four types of light stimulation: white (5600 K), blue (450 nm), green (510 nm) and red (600 nm). The basal diameter of the pupil increased significantly for alcohol concentrations equal to or greater than 0.25 mg/l in exhaled breath. Moreover, the value of the amplitude for red light constriction also provided

significant differences between the two conditions. These results are promising in the search for new methods to detect illegal alcohol levels among drivers. This study demonstrates that basal pupil diameter increase and amplitude response could be used as an alcohol consumption level indicator. However, further studies are necessary to validate this and other diagnose methods complementary to breathalyzer and other drugs tests.

## 2.6 Pupillometers

The medical industry is evolving rapidly in the past decade regarding the field of pupillometry. There is a variety of pupillometers available for purchase, each one containing a different total of features, according to the purpose for which it was designed.



Figure 6 : DIGITAL PUPILLOMETER / HAND-HELD PD-82 II

Most pupillometers report the pupil's radius and rely on the examiner to provide the stimulus and appropriate environmental lighting.

Cutting edge pupillometers, such as the one designed during this project, provide the appropriate lighting and can be used under any setting.

A pupillometer's main purpose is to:

- Provide a dark setting so that the pupil can fully dilate.
- Record and store a video of the pupil during the examination.

- Locate and measure the pupil with the minimum possible error.
- Stimulate the pupil using a Light Emitting Diode (LED) or other safe light emitters.
- Provide statistics and metrics regarding the Pupillary Light Reflex.

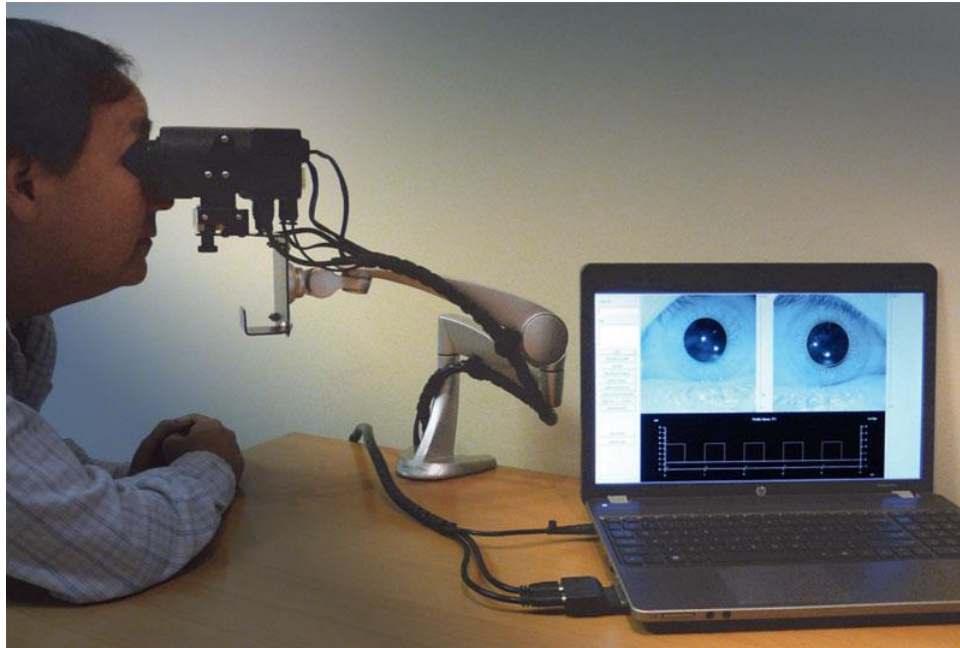


*Figure 7: PC-based Desktop Pupillometer with 4-color stimulus*

## Part 3: Our custom pupillometer

For the purpose of this project, we (the optics and biotechnology team of Technical University of Crete) decided to create our own pupillometer. What distinguishes our work from the existing commercial devices is a unique set of features, such as using 12 different monochromatic LEDs as stimulus and providing a complete wireless and portable solution. The full list of features will be provided below.

### 3.1 List of Hardware Features

Our device has covered a unique set of features. Most of them are covered below:

- Fully portable solution, but a Wi-Fi enabled PC is required.
- Wi-Fi enabled, completely wireless.
- Rechargeable, with up to 7 hours of use.
- 2 Raspberry Pi Cameras, one for each eye.
- 1 Raspberry Pi Zero W.
- 1 Raspberry Pi Zero.
- 11 Monochromatic LEDs and 1 White LED, 2 for each eye (48 total)
- 4 Infrared LEDs for backlight illumination, 2 for each eye.

### 3.2 Components

#### 3.2.1 Raspberry Pi Zero W

The Raspberry Pi Zero W is a small integrated device with significant computational power and low energy consumption. The RPi Zero W is responsible for four main operations:

- a) Encoding video from the left Raspberry Pi Camera to h.264\*.
- b) Sending encoded video feed to a Wi-Fi enabled PC.
- c) Receiving commands from the PC.
- d) Executing commands (toggling LEDs and setting the cameras)

These functions were implemented by our optics team's software engineers.

*\*The intent of the H.264/AVC project was to create a standard capable of providing good video quality at substantially lower bit rates than previous standards (i.e., half or less the bit rate of MPEG-2, H.263, or MPEG-4 Part 2), without increasing the complexity of design so much that it would be impractical or excessively expensive to implement. Our project requires high quality in low bitrates, so H.264 was the optimal solution.*



*Figure 8: Raspberry Pi Zero W*

The Raspberry Pi Zero W extends the Pi Zero family. Launched at the end of February 2017, the Pi Zero W has all the functionality of the original Pi Zero, but comes with added connectivity, consisting of:

- 802.11 b/g/n wireless LAN
- Bluetooth 4.1
- Bluetooth Low Energy (BLE)

Like the Pi Zero, it also has:

- 1GHz, single-core CPU
- 512MB RAM
- Mini HDMI and USB On-The-Go ports
- Micro USB power
- HAT-compatible 40-pin header
- Composite video and reset headers
- CSI camera connector

### 3.2.2 Raspberry Pi Zero

The second Raspberry Pi is only needed for encoding the right camera's video feed. Consequently, a smaller, less demanding device had to be used. The Raspberry Pi Zero is the perfect candidate, as it saves space, energy and cost without cutting performance.

The Raspberry Pi Zero is half the size of a Model A+, with twice the utility. A tiny Raspberry Pi that's affordable. Specifications:

- 1GHz single-core CPU
- 512MB RAM

- Mini HDMI port
- Micro USB OTG port
- Micro USB power
- HAT-compatible 40-pin header
- Composite video and reset headers
- CSI camera connector (v1.3 only)



*Figure 9: Raspberry Pi Zero*

### 3.2.3 USB Connection

In order to retrieve the video feed from the right eye camera (Raspberry Pi Zero), a USB Connection had to be implemented that connects the RPi Zero to the RPi Zero W. By connecting the USB RX/TX ports with a cable similar to the figure below and creating a network interface “usb0” using a static IP, we managed to transfer the data using the following pathway: a) the right camera captures the video, b) the video is encoded to h.264, c) the encoded video is sent to RPi Zero W via USB, d) the encoded video reaches the computer via Wi-Fi.



*Figure 10: USB Mini-B to USB Mini B cable*

### 3.2.3 Raspberry Pi Camera

The Raspberry Pi Camera Module v2 comes with a Sony IMX219 8-megapixel sensor.



Figure 11: Raspberry Pi Camera

We chose to use this module due to its compatibility with the Raspberry Pi. Moreover, thanks to Sony's Exmor-RS Backlight Illumination, we get high quality video under low light conditions.

Technical Specifications:

<b>Size</b>	Around $25 \times 24 \times 9$ mm
<b>Weight</b>	3g
<b>Still resolution</b>	8 Megapixels
<b>Video modes</b>	1080p30, 720p60 and $640 \times 480$ p60/90
<b>Linux integration</b>	V4L2 driver available
<b>C programming API</b>	OpenMAX IL and others available
<b>Sensor</b>	<a href="#">Sony IMX219</a>
<b>Sensor resolution</b>	$3280 \times 2464$ pixels
<b>Sensor image area</b>	$3.68 \times 2.76$ mm (4.6 mm diagonal)
<b>Pixel size</b>	$1.12 \mu\text{m} \times 1.12 \mu\text{m}$
<b>Optical size</b>	1/4"
<b>Full-frame SLR lens equivalent</b>	35 mm
<b>S/N ratio</b>	36 dB
<b>Dynamic range</b>	67 dB @ 8x gain
<b>Sensitivity</b>	680 mV/lux-sec

<b>Dark current</b>	16 mV/sec @ 60 C
<b>Well capacity</b>	4.3 Ke-
<b>Fixed focus</b>	1 m to infinity
<b>Focal length</b>	3.04 mm
<b>Horizontal field of view</b>	62.2 degrees
<b>Vertical field of view</b>	48.8 degrees
<b>Focal ratio (F-Stop)</b>	2.0

### 3.2.4 Optical Filters

The camera's video feed is constituted solely by infrared radiation. During the eye's stimulation with monochromatic or white LEDs, there is obsolete light that adds noise to the video feed, such as extra brightness and small mirrored spots on the pupil that impair the pupil detection.

The solution to the above problem was to add an infrared optical filter for each eye. The Monochromatic and White LED frequencies are cut-off and all that remains is a crystal clear video of the eye.

### 3.2.5 Light diffuser

The eyes are very sensitive to light exposure and must be protected at all cost. In order to create an ambient lighting environment we added a thick disc that diffuses the light so that the examinee's eyes don't get hurt during the process, whilst getting more smoothly accommodated to the change in the lighting of the environment.

The diffusers are thick semi-transparent discs made of acrylic (plexi-glass).

In the figure below, we can see the light diffuser (white disc) and the black IR-Pass optical filter in the middle.

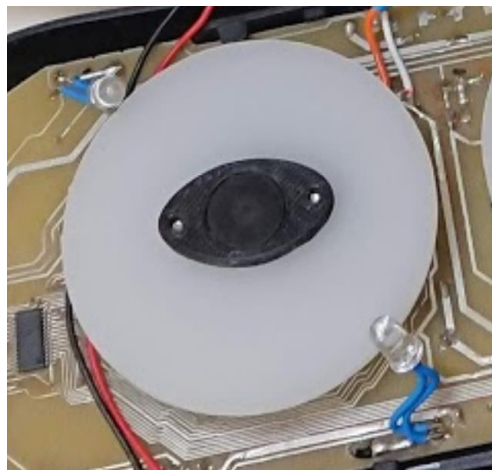


Figure 12: Light diffuser and Optical filter

### 3.2.6 Light Emitting Diodes (LEDs)

This device contains 11 different monochromatic LED types and 2 white LED types. For each eye we added two LEDs of each color, so we get a total of 12 colors \* 2 eyes \* 2 LEDs/eye = 48 LEDs.

For backlight illumination we chose to use infrared LEDs. Infrared radiation can't stimulate the human eye and can be seen by most cameras.

The LEDs intensities were normalized using a photometer. By normalizing the LED intensities, we are certain that the <Eye Diameter vs Time> graph is not biased on any wavelength. According to many scientific papers on Pupillary Light Reflex, the light's intensity is proportional to the constriction percentage.

In order to normalize the luminous intensity of every LED, we initially recorded every intensity at its peak wavelength. We discovered that some LEDs are not as bright as others, so the normalization value had to be the minimum value when every LED is on 100% output. The minimum value was  $30\mu\text{W}$  at **peak wavelength**. This means that the actual radiant luminosity of every LED is higher than this value.

We also calculated and printed every LED's spectrum using a spectrometer. The result can be seen below, for every LED.

The chart below proves that the constricted pupil diameter is a function of radiant luminosity [11]:

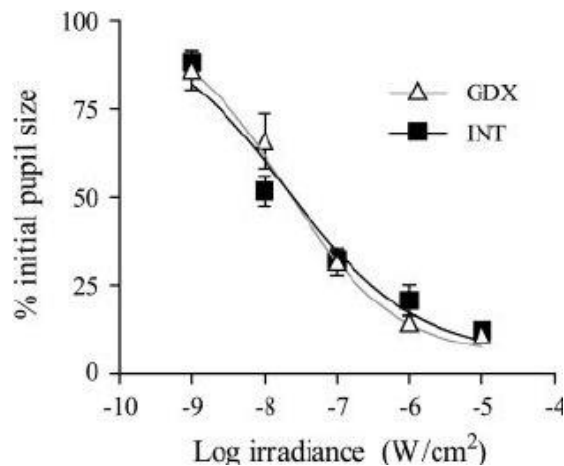


Figure 13: Androgenic effects on PLR.

## Monochromatic LEDs

### 430 nm

The first LED type is borderline blue-violet radiation, but appears blue to the eye. Model number: CMD15- 21UBC/TR8.

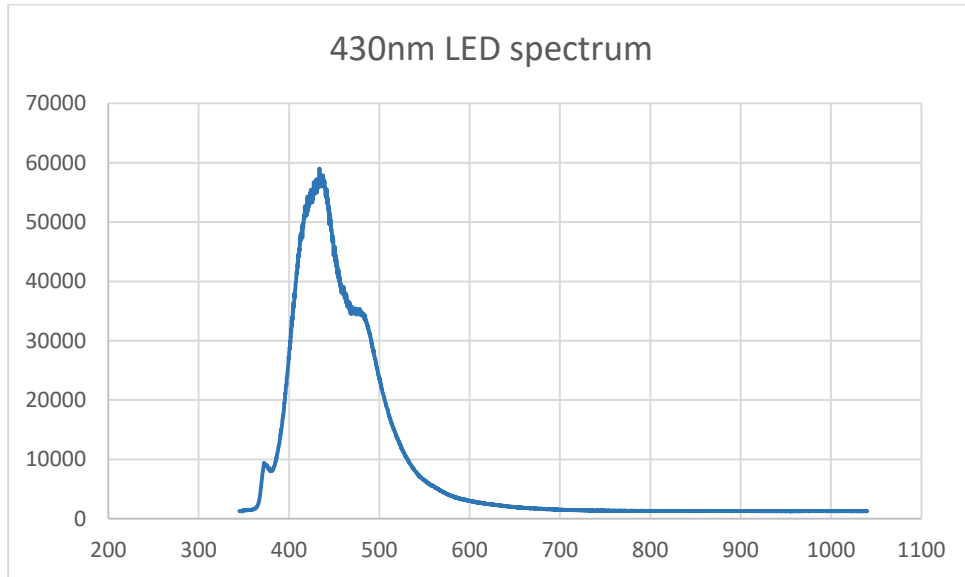


Figure 14: 430nm LED full spectrum. (Intensity vs wavelength in nm)

Specifications:

Parameter	Value
<b>Illumination Color:</b>	Blue
<b>Wavelength/Color Temperature:</b>	430 nm
<b>Luminous Intensity:</b>	45 mcd
<b>Viewing Angle:</b>	140 deg
<b>Lens Color/Style:</b>	Water Clear
<b>If - Forward Current:</b>	20 mA
<b>Vf - Forward Voltage:</b>	4.9 V



Figure 15: 430nm LED

### 460 nm

The second LED type belongs to the blue radiation spectrum. Model number: LD MVSGJGLH-46-1.

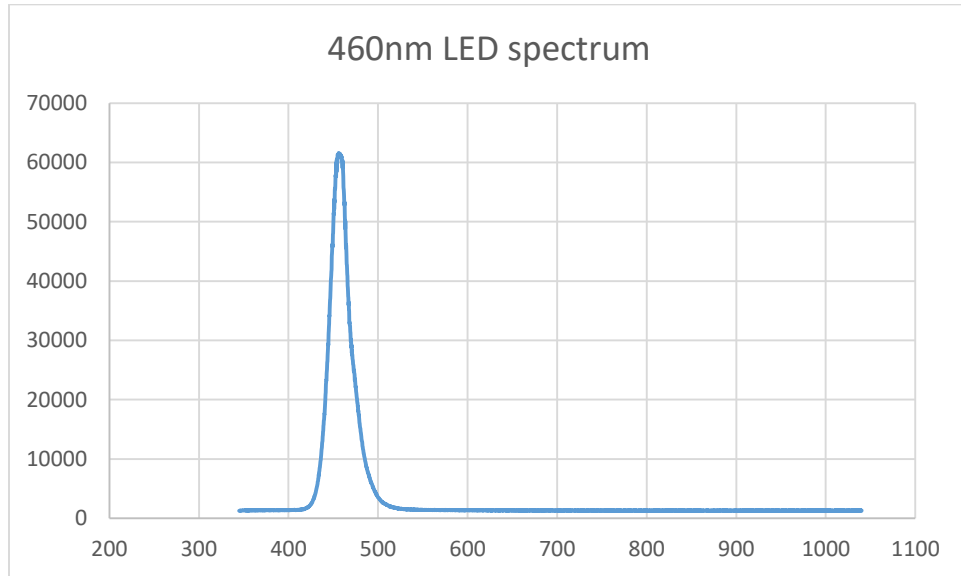


Figure 16: 460nm LED full spectrum. (Intensity vs wavelength in nm)

Specifications:

Parameter	Value
Color	Blue
Wavelength	459nm (453nm ~ 465nm)
Current Test	20mA
Voltage – Forward (Vf) (Typ)	3.05V
Max Current	30mA



Figure 17: 460nm LED

## 470 nm

The third LED type belongs to the blue radiation spectrum. Model number: LB Q39G-L2OO-35-1.

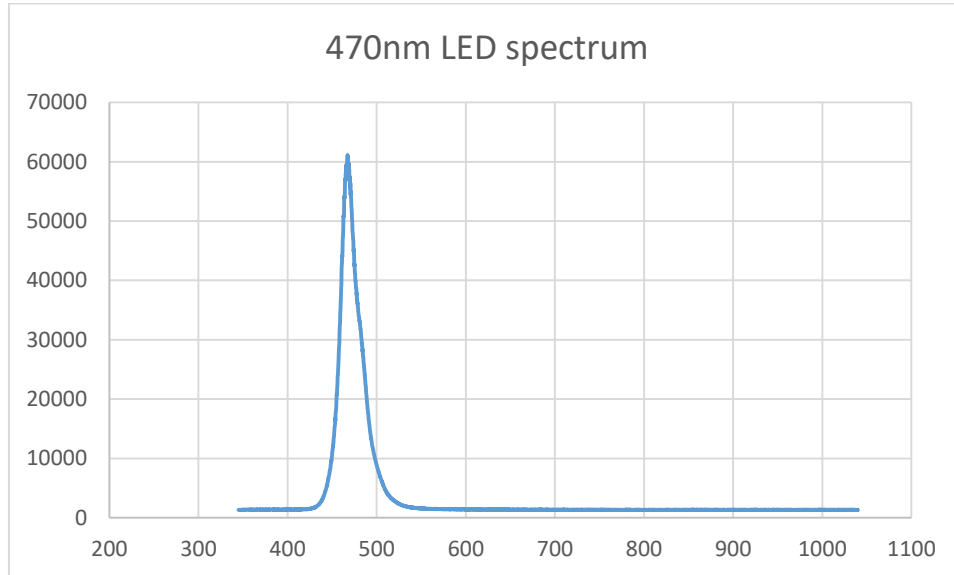


Figure 18: 470nm LED full spectrum. (Intensity vs wavelength in nm)

Specifications:

Parameter	-	Values
Peak Wavelength	typ.	465 nm
Dominant Wavelength	typ.	470 nm
Spectral Bandwidth at 50% $I_{rel,max}$	typ.	22 nm
Viewing angle at 50 % $I_V$ values for 0°, 90°	typ.	170 ° 130 °
Forward Voltage $I_F = 5 \text{ mA}$	typ. max.	2.85 V 3.10 V
Reverse current $V_R = 5 \text{ V}$	typ. max.	0.01 $\mu\text{A}$ 10 $\mu\text{A}$



Figure 19: 470nm LED

## 515 nm

The fourth LED type belongs to the green radiation spectrum. Model number: AA3021ZGSK.

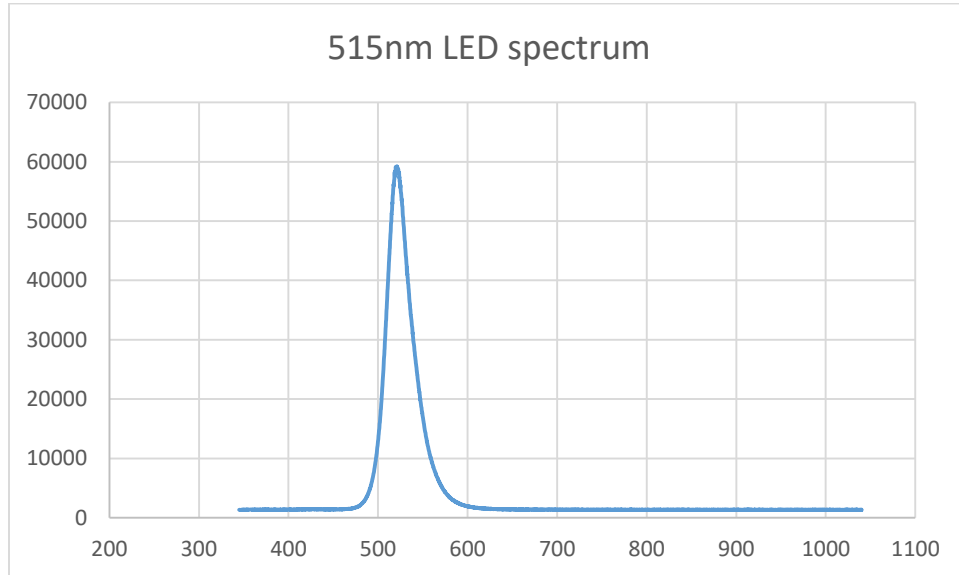


Figure 20: 515nm Full Spectrum (Intensity vs wavelength in nm)

Specifications:

Parameter	Values
Peak Wavelength	515 nm
Dominant Wavelength	525 nm
Spectral Bandwidth at 50% $I_{rel,max}$	36 nm
Viewing angle	120 °
Forward Voltage (typ.)	3.3 V
$I_F = 5 \text{ mA (max.)}$	4.1 V
Reverse current (max.)	50 $\mu\text{A}$
$V_R = 5 \text{ V}$	



Figure 21: 515nm LED

### 535 nm

The fifth LED type belongs to the green radiation spectrum. Model number: APT1608VGC/Z-PRV.

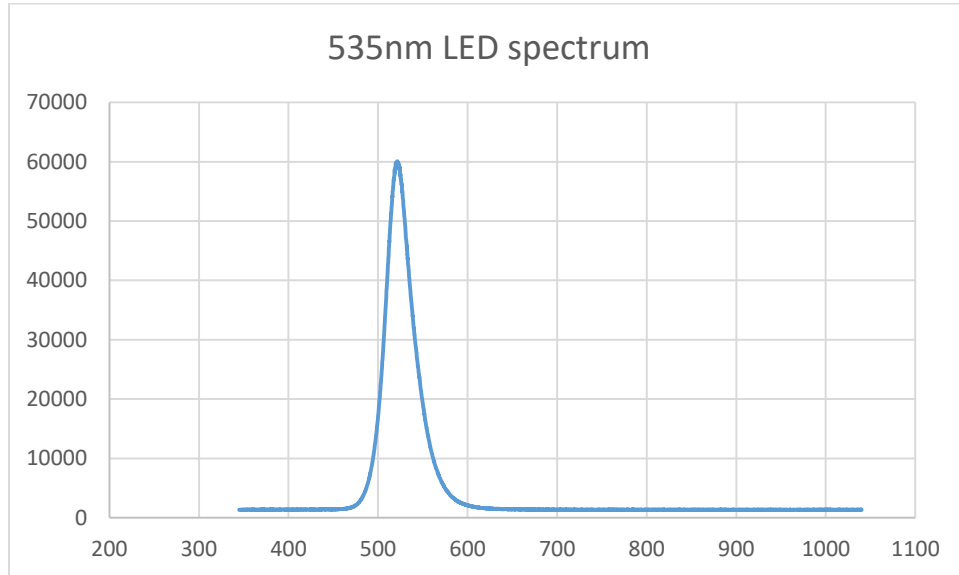


Figure 22: 535nm LED spectrum (Intensity vs wavelength in nm)

Specifications:

Parameter	Device	Typ.	Max.	Test Conditions
Peak Wavelength	Green	525 nm		IF=20mA
Dominant Wavelength	Green	535 nm		IF=20mA
Spectral Line Half-width	Green	39 nm		IF=20mA
Forward Voltage	Green	3.2	3.7 V	IF=20mA
Reverse Current	Green		10 $\mu$ A	VR=5V



Figure 23: 535nm LED

## 569 nm

The sixth LED type belongs to the green radiation spectrum. Model number: LTSTC190GKT.

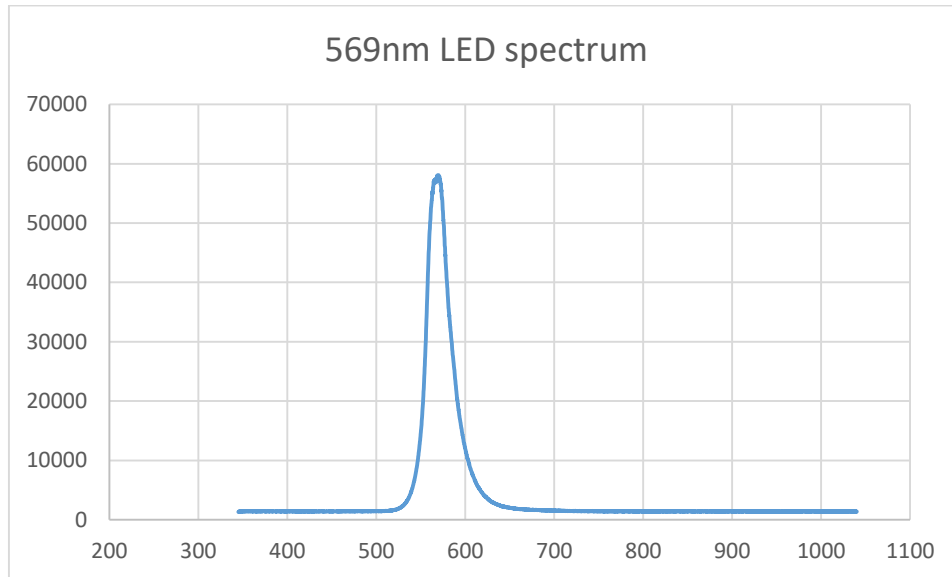


Figure 24: 569nm LED spectrum (Intensity vs wavelength in nm)

Specifications:

Parameters	Values
Wavelength/Color Temperature	569 nm
Luminous Intensity	6 mcd
Viewing Angle	130 °
Lens Color/Style	Water Clear
If - Forward Current	20 mA
Vf - Forward Voltage	2.1 V



Figure 25: 569nm LED

## 587 nm

The seventh LED type belongs to the borderline yellow-orange radiation spectra. Model number: LY L29K-H1K2-26-Z.

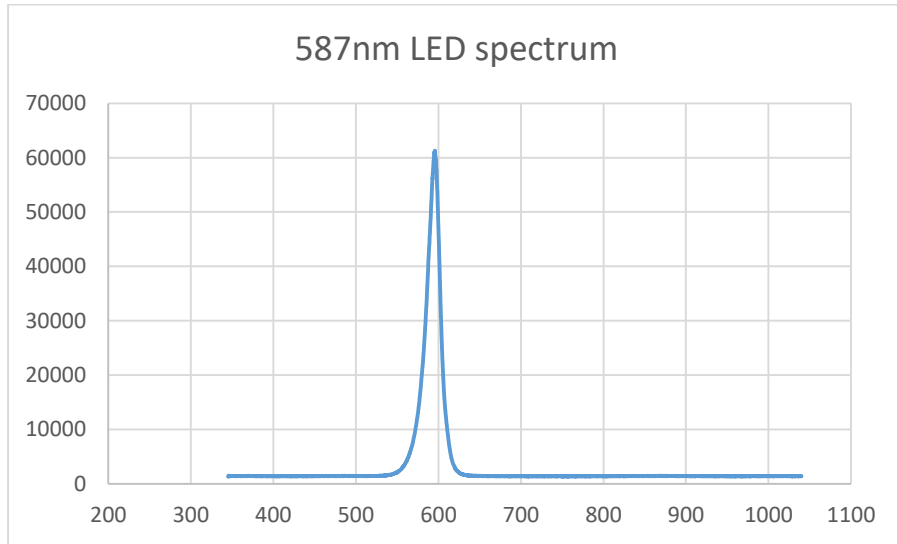


Figure 26: 587nm LED spectrum (Intensity vs wavelength in nm)

Specifications:

Parameter	Values
Wavelength at peak emission (typ.)	591 nm
Dominant Wavelength (typ.)	587 nm
Spectral bandwidth at 50% $I_{rel}$ max (typ.)	15 nm
Viewing angle at 50 % $I_V$ (typ.)	160 °
Forward voltage ( $I_F = 20$ mA) (typ.) (max.)	1.80 V
Reverse current ( $V_R = 12$ V) (typ.)	0.01 $\mu$ A

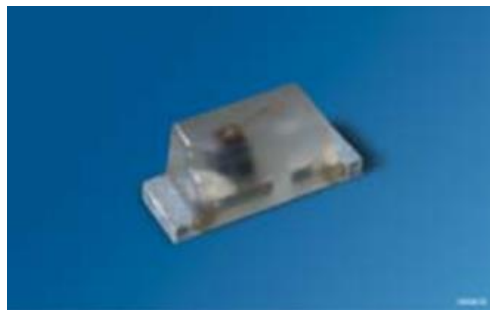


Figure 27: 587nm LED

## 605nm

The eighth LED type belongs to the orange radiation spectrum. Model number: LO Q976-PS-25.

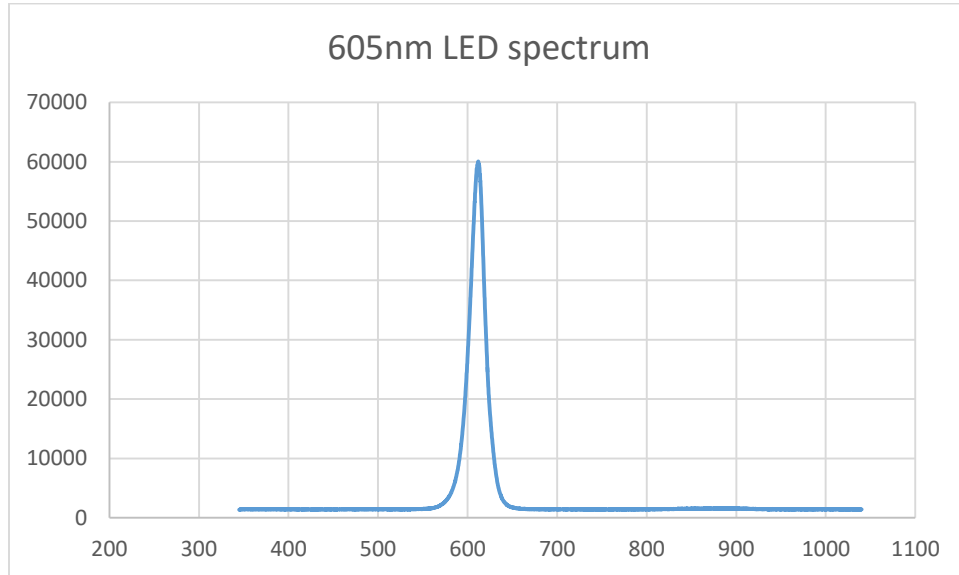


Figure 28: 605nm LED Full Spectrum (Intensity vs wavelength in nm)

Specifications:

Parameter	Values
Wavelength at peak emission (typ.)	610 nm
Dominant Wavelength (typ.)	605 nm
Spectral bandwidth at 50% $I_{rel}$ max (typ.)	16 nm
Viewing angle at 50 % $I_V$ (typ.)	160 °
Forward voltage ( $I_F = 20$ mA) (typ.)	2.00 V
(max.)	2.50 V
Reverse current ( $V_R = 12$ V) (typ.)	0.01 $\mu$ A



Figure 29: 605nm LED

## 645 nm

The ninth LED type belongs to the borderline orange-red radiation spectra. Model number: LH R974-LP-1.

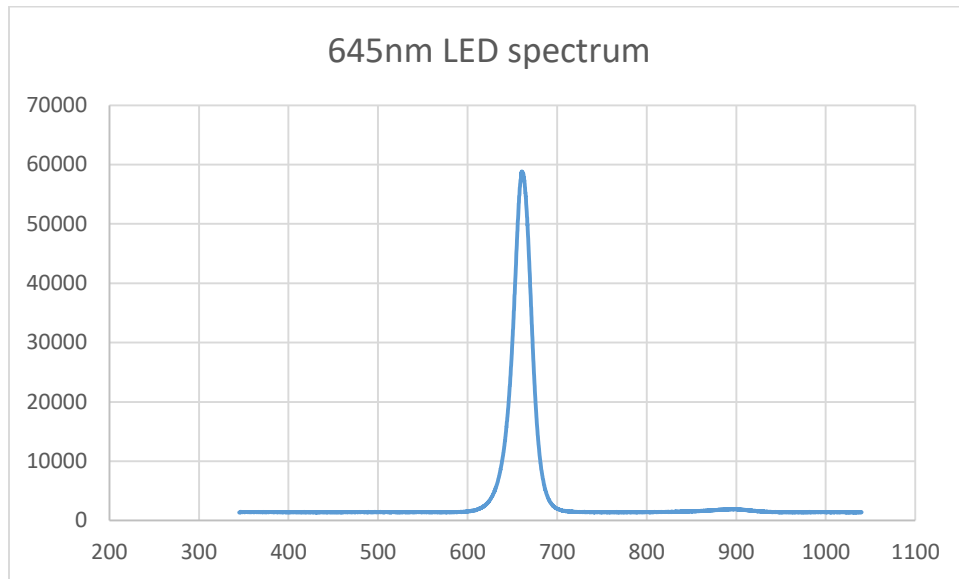


Figure 30: 645nm LED Full Spectrum (Intensity vs wavelength in nm)

Specifications:

Parameter	Values
Wavelength at peak emission (typ.)	660 nm
Dominant Wavelength (typ.)	645 nm
Spectral bandwidth at 50% $I_{rel}$ max (typ.)	20 nm
Viewing angle at 50 % $I_V$ (typ.)	160 °
Forward voltage ( $I_F = 20$ mA) (typ.)	1.80 V
(max.)	2.60 V
Reverse current ( $V_R = 5$ V) (typ.)	0.02 $\mu$ A
(max.)	100 $\mu$ A



Figure 31: 645nm LED

**700 nm**

The tenth LED type belongs to the red radiation spectrum. Model number: SML-LX15HC-RP-TR.

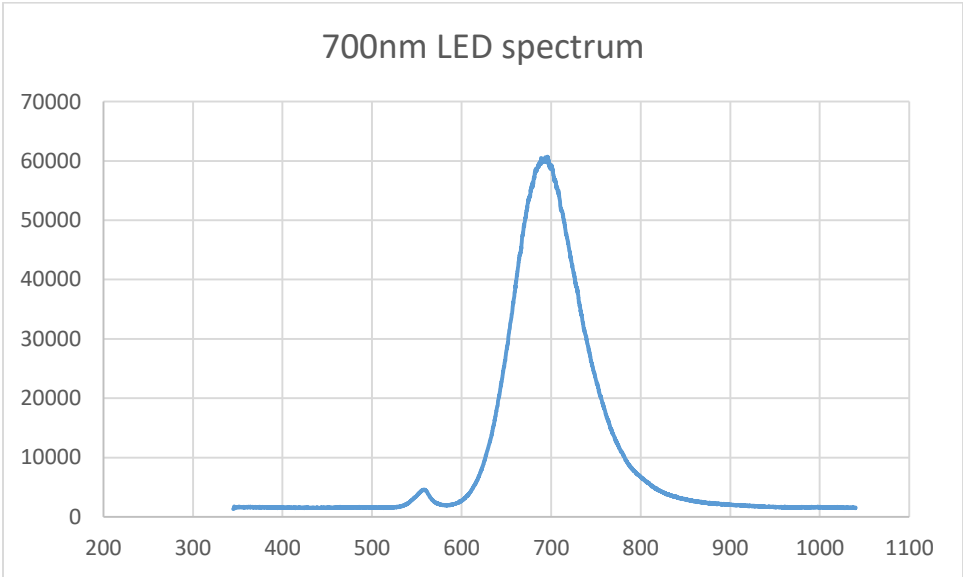


Figure 32: 700nm LED Full Spectrum (Intensity vs wavelength in nm)

Specifications:

Parameter	Values
Wavelength at peak emission (typ.)	700 nm
Viewing angle at 50 % I <sub>V</sub> (typ.)	140 °
Forward voltage (I <sub>F</sub> = 20 mA) (typ.)	2.00 V
(max.)	2.50 V
Reverse current (V <sub>R</sub> = 5 V) (typ.)	10 μA



Figure 33: 700nm LED

## 730 nm

The eleventh LED type belongs to the borderline red – infrared radiation spectra (Far Red spectrum).  
Model number: XPEFAR-L1-0000-00601.

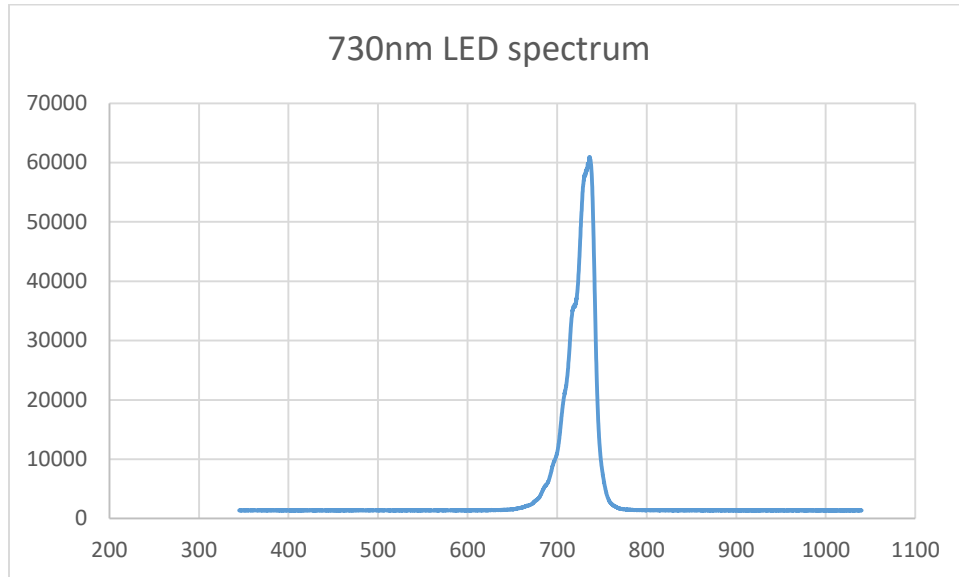


Figure 34: 730nm LED Full Spectrum (Intensity vs wavelength in nm)

Specifications:

Parameter	Values
Wavelength at peak emission (typ.)	730 nm
Viewing angle at 50 % $I_V$ (typ.)	115-130 °
Forward voltage ( $I_F = 20$ mA) (typ.)	3.25 V
(max.)	3.5 V
Forward current ( $V_R = 5$ V) (max.)	1000 mA

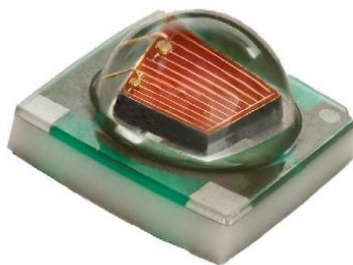


Figure 35: 730nm LED

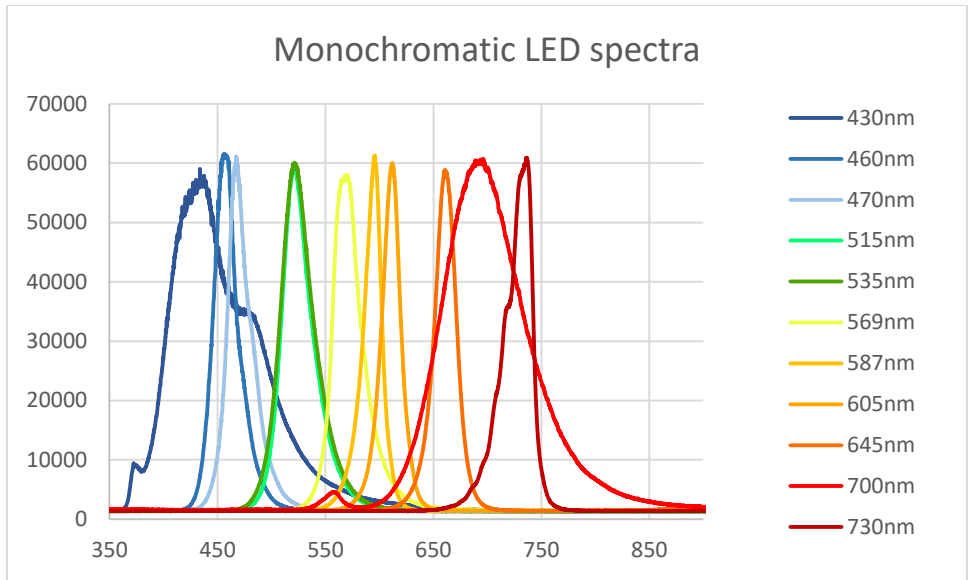


Figure 36: Monochromatic LED spectra (Intensity vs wavelength in nm)

*White LEDs*

The twelfth type is a mix of warm and cold white. We chose to mix these LED types in order to achieve a true white color. Both LEDs peak near the orange and blue radiation spectra. The warm has higher intensities near red, whereas the cold one has higher intensities near blue. Model: Nichia 157AT.

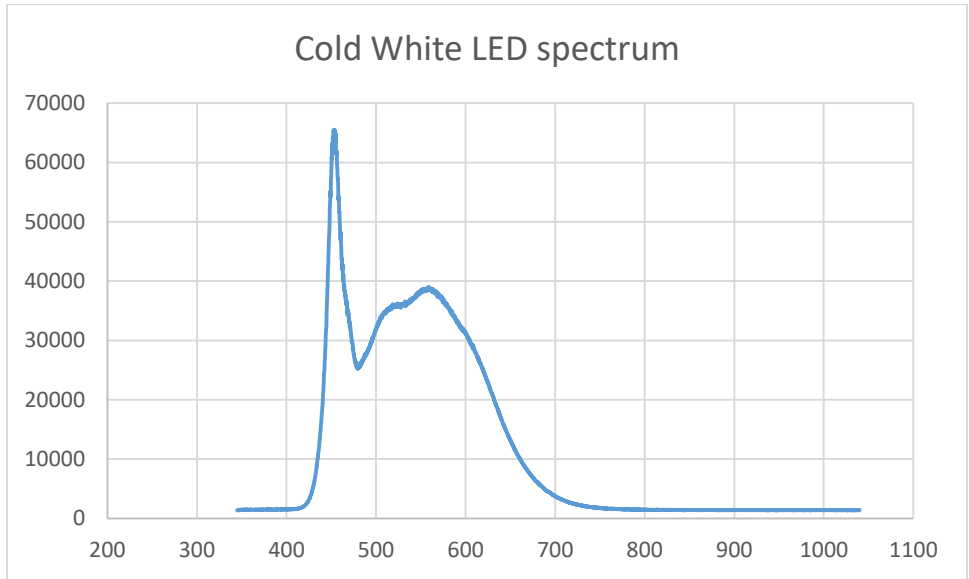


Figure 37: Cold White LED Full Spectrum

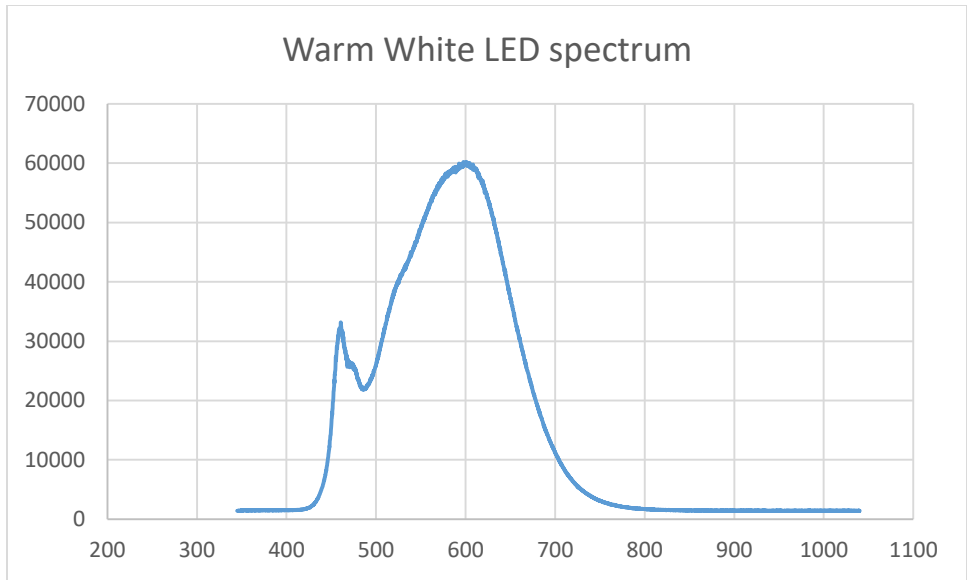


Figure 38: Warm White LED Fill Spectrum

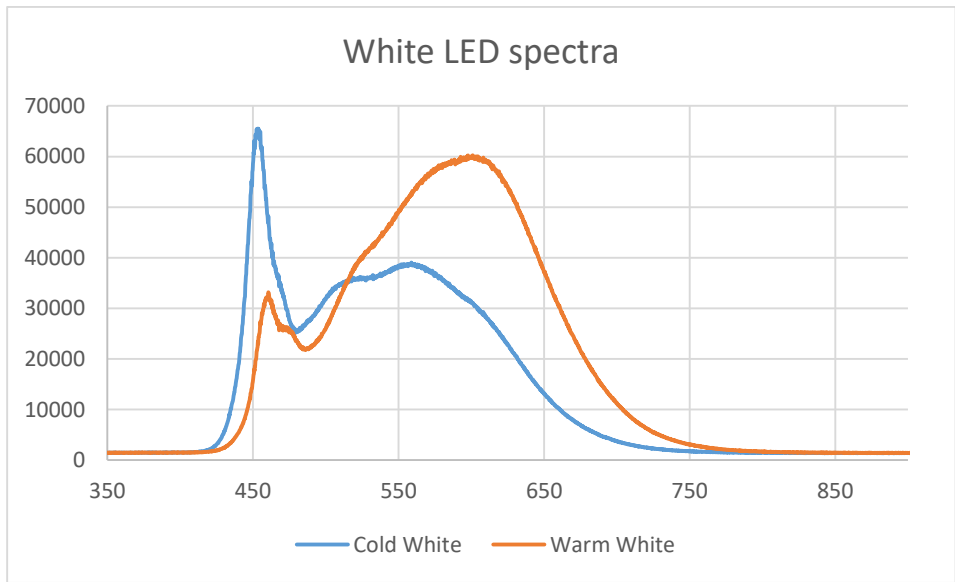


Figure 39: Final (True White) white LED combination

Specifications:

Forward Current (max) : 150mA.



Figure 40: White LED

### Infrared LEDs

The Infrared LEDs are used for environment illumination.

Their intensities were calculated according to the IEC-62471 Standard, using the Intersil Eye Safety Calculator [13].

The maximum emission allowed by the above health regulations is  $0.01 \text{ W/cm}^2$ . The IR LEDs are preset below that value, never reaching values above  $0.008 \text{ W/cm}^2$ .

Specifications:

Symbol	Value
<b>Radiant Intensity (mW/sr)</b>	7.8
<b>Viewing Angle (deg)</b>	30
<b>Spectral Bandwidth (nm)</b>	45
<b>Peak Emission Wavelength (nm)</b>	850



Figure 41: Infrared LEDs

### 3.2.7 Arduino Nano

The Arduino Nano is a small, complete, and breadboard-friendly board based on the ATmega328 (Arduino Nano 3.x). The Arduino Nano was preferred in our project due to its low cost and high fidelity on handling analog signals. The Arduino Nano receives commands from the Raspberry Pi Zero W and executes them. Its main function is toggling LEDs.

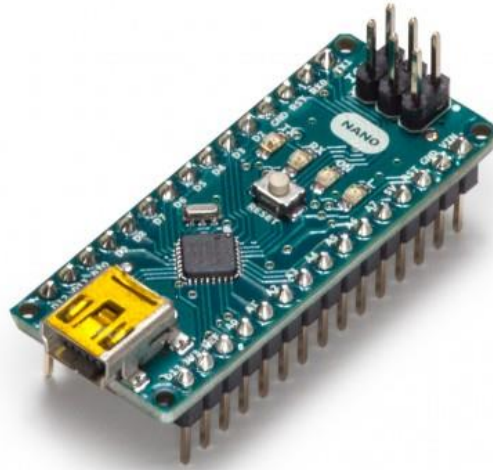


Figure 42: Arduino Nano

Technical Specifications:

<b>Microcontroller</b>	ATmega328
<b>Architecture</b>	AVR
<b>Operating Voltage</b>	5 V
<b>Flash Memory</b>	32 KB of which 2 KB used by boot loader
<b>SRAM</b>	2 KB
<b>Clock Speed</b>	16 MHz
<b>Analog IN Pins</b>	8
<b>EEPROM</b>	1 KB
<b>DC Current per I/O Pins</b>	40 mA (I/O Pins)
<b>Input Voltage</b>	7-12 V
<b>Digital I/O Pins</b>	22 (6 of which are PWM)
<b>PWM Output</b>	6
<b>Power Consumption</b>	19 mA
<b>PCB Size</b>	18 x 45 mm
<b>Weight</b>	7 g

### 3.2.8 LED Controller

Besides the Arduino Nano, we used a TLC5940 that assists us in turning LEDs on and off. While the Arduino Nano is the device that handles the analog signals responsible for toggling LEDs, the TLC is key at controlling Pulse Width Modulations (PWMs).



Figure 43: TLC 5940

Technical Specifications:

<b>Channels</b>	16
<b>PWM Control</b>	12 bit (4096 Steps) Grayscale PWM Control
<b>Dot Correction</b>	6 bit (64 Steps) Storable in Integrated EEPROM
<b>Drive Capability (Constant-Current Sink)</b>	0 mA to 60 mA (VCC < 3.6 V) 0 mA to 120 mA (VCC > 3.6 V)
<b>LED Power Supply Voltage</b>	up to 17 V
<b>VCC</b>	3 V to 5.5 V
<b>Serial Data Interface</b>	Yes
<b>Controlled In-Rush Current</b>	Yes
<b>Data Transfer Rate</b>	30 MHz
<b>CMOS Level</b>	I/O
<b>Error Information</b>	LOD: LED Open Detection TEF: Thermal Error Flag

### 3.2.9 Hull

All of the components were inserted into an empty VR Mask. The purpose of the chosen VR Mask was inserting a smartphone in order to experience a Virtual Reality setting. For the purposes of this project, the mask was completely emptied of its contents and the empty hull was filled with a motherboard containing all of the above components, soldered onto specific positions.

A big part of the shell was filled with high fidelity batteries, lasting up to 7 hours of use. The shell also features an on/off switch and a battery indicator. A boost converter (3.7 to 5 V, min. 2A) was also used to power the system. The batteries can be charged with a 5V smartphone charger.

Another challenge that we had to overcome is the light that leaks into the device. The effect was not catastrophic, but it definitely reduced the image quality. To overcome this problem we had a custom cloth sown for the device. The custom made cloth is shown below. The cloth is 100% polyester, which blocks all the external polluting radiation.



*Figure 44: The shell of the device*



*Figure 45: Light eliminating cloth*



*Figure 46: Inside the device*



*Figure 47: Top View of the Device*



*Figure 48: Rear View of the Device*

### 3.3 Schematics

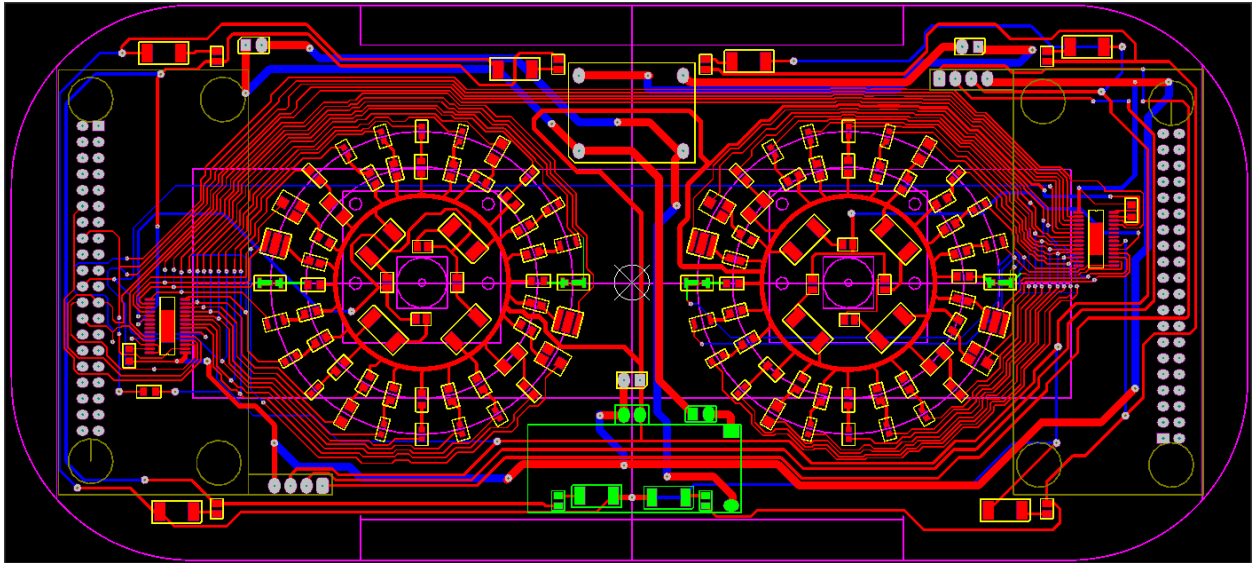


Figure 49: Motherboard Schematics [Low Level]

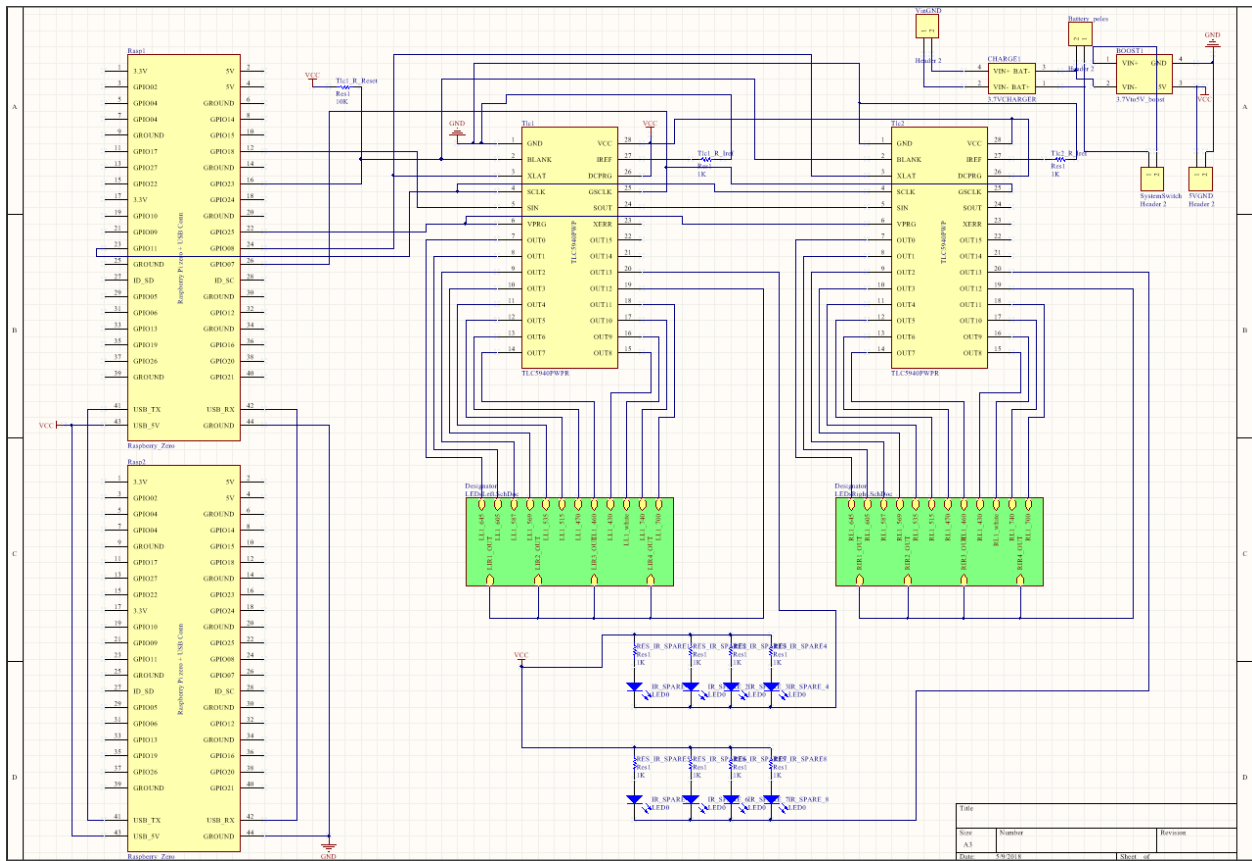


Figure 50: Motherboard Schematics [Top Level]

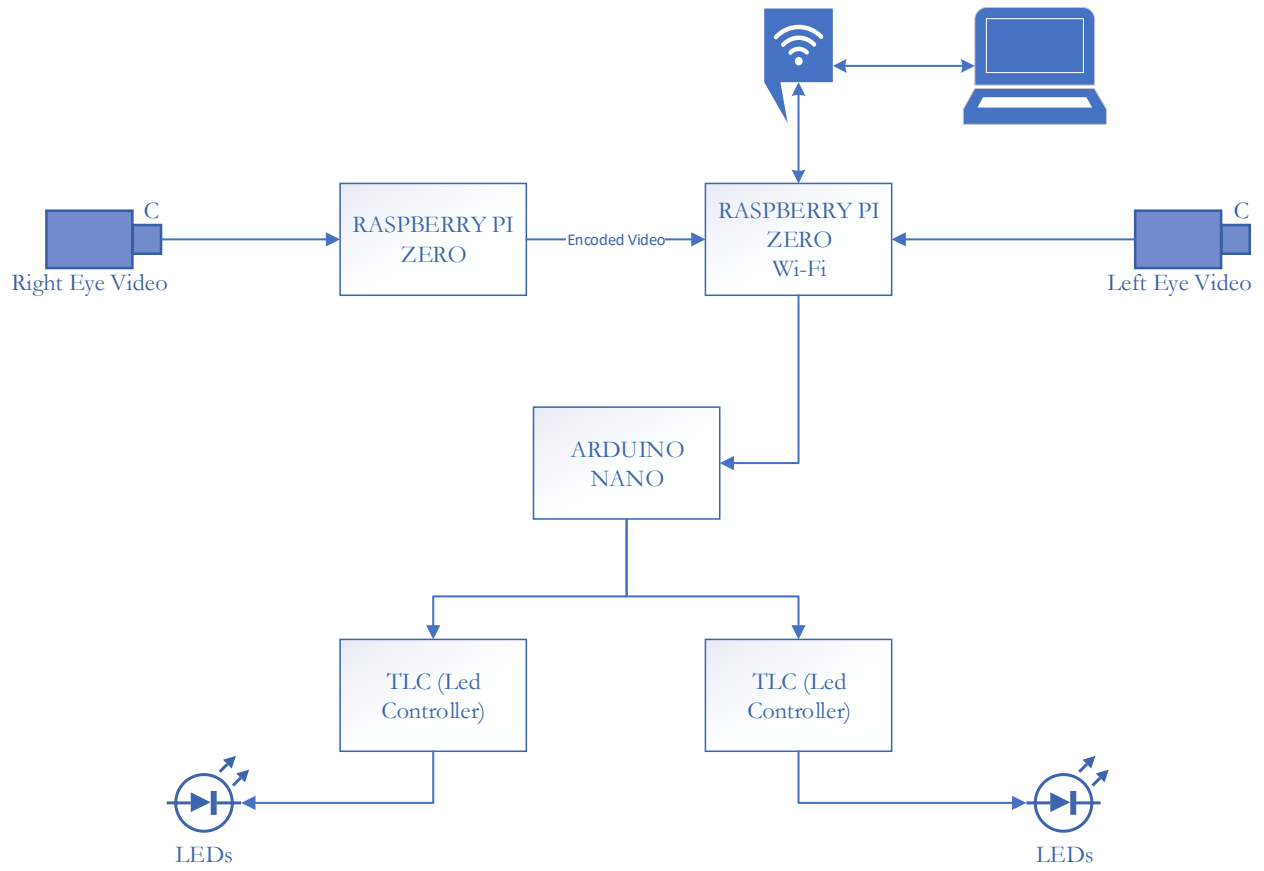


Figure 51: Hardware Flowchart

## Part 4: Software

The main objective of this thesis is to design a Graphical User Interface (GUI) that is fast, easy to use and highly detailed. Aside from the GUI, there are several algorithms and complicated functions on the backend, which will be explained in detail below.

This project was built on the Qt Platform using an LGPL license. C++ was used as programming language. C++ is widely preferred amongst scientists and engineers due to its flexibility, speed and reliability. Some external libraries were used to assist the video decoding and GUI aesthetics.

### 4.1 Graphical User Interface

The first part of the software is the GUI. A GUI is a type of user interface that allows users to interact with electronic devices through graphical icons and visual indicators such as secondary notation, instead of text-based user interfaces, typed command labels or text navigation.

#### 4.1.1 Examinee's profile

The "Patient Profile" menu provides all the info about our patient. This info is stored in a database. The menu contains the following info:

- Full Name and Age
- Contact Info
- Gender
- Physical Condition of the body (fitness)
- Known neurological or psychological conditions

The fields "Gender", "Fitness" and "Known Conditions" may assist us in extracting conclusions after an ample number of samples has been collected. It is proven by many papers that women have different pupil sizes than men. Fitness is also a factor that has to be taken into consideration, since body exercise ameliorates both our reflexes and cognitive function.

The most important field in this page though, is the field "Known Conditions". Should a pattern be spotted in the future in e.g. all "Alzheimer's" patients, then pupillometry may be proven to be key in recognizing and diagnosing neurological diseases, such as Alzheimer's and Parkinson's. Scientific literature has already linked Alzheimer's and Parkinson's with abnormal PLR.

In order to achieve the above, a vast number of samples has to be retrieved in both normal and diseased individuals.

**Pupillometry**

**PATIENT PROFILE**

Firstname: Anastasis

Lastname: Chatzioannou

Birthday: 06-12-2095

e-mail: achatzioannou@hotmail.com

Phone: 6976663855

Gender:  Male  Female

Fitness: [Slider]

Known Conditions:

- Alzheimer's
- Parkinson's

- Autism
- Coma
- Brain injury
- Dementia
- Use of opiates
- Use of marijuana
- Generalized anxiety disorder
- Depression

Save

Figure 52: Examinee's profile.

#### 4.1.2 Lists of Patients and Examinations

Below we can see the menus “List of all patients” and “List of patient’s examinations”.

List of all patients: In order to select a patient we click anywhere on the row that contains his/her name. After selecting the patient, the 3 buttons on the right will activate.

We can then a) edit his profile, b) see his past examinations, c) start a new examination.

A new patient may be registered using the “New Patient” button.

List of patient’s examinations: In order to select an examination we click anywhere on the row that contains its date and time. After selecting the examination, the 2 buttons on the right will activate.

We can then a) view the examination, b) delete the examination.

Both menus contain a search bar that will refine the table’s contents according to the filter we use. For example by typing “23” we can instantly see all the examinees in the age of 23.

Pupillometry

New patient

Type a name to search...

Firstname	Lastname	Email	Phone	Age	Gender	Fitness (1-10)
Anastasis	Chatzioannou	achatzioannou@hotmail.com	6976663855	23	M	7
Ellie	Skourtanioti			23	F	7
Dimitris	Markellos			32	M	7

Edit  
Examinations  
New examination

Figure 53: List of patients

Pupillometry

Examination list for : Anastasis Chatzioannou

	Exam date	Examiner
1	17/07/2018 13:06	Anastasis Chatzioannou
2	17/07/2018 13:10	Anastasis Chatzioannou
3	17/07/2018 13:12	Anastasis Chatzioannou
4	17/07/2018 13:19	Anastasis Chatzioannou
5	17/07/2018 13:21	Anastasis Chatzioannou
6	17/07/2018 13:22	Anastasis Chatzioannou
7	17/07/2018 13:29	Anastasis Chatzioannou
8	18/07/2018 13:22	Anastasis Chatzioannou
9	18/07/2018 13:22	Anastasis Chatzioannou
10	18/07/2018 14:30	Anastasis Chatzioannou
11	18/07/2018 14:31	Anastasis Chatzioannou
12	18/07/2018 14:34	Anastasis Chatzioannou
13	23/07/2018 12:15	Anastasis Chatzioannou
14	26/07/2018 11:48	Anastasis Chatzioannou
15	26/07/2018 12:01	Anastasis Chatzioannou
16	26/07/2018 12:05	Anastasis Chatzioannou
17	30/07/2018 13:41	Anastasis Chatzioannou

View  
Delete

Figure 54: List of exams.

### 4.1.3 Review Examination Menu

In this menu we are able to review an examination's results. Here is an overview of the whole page:

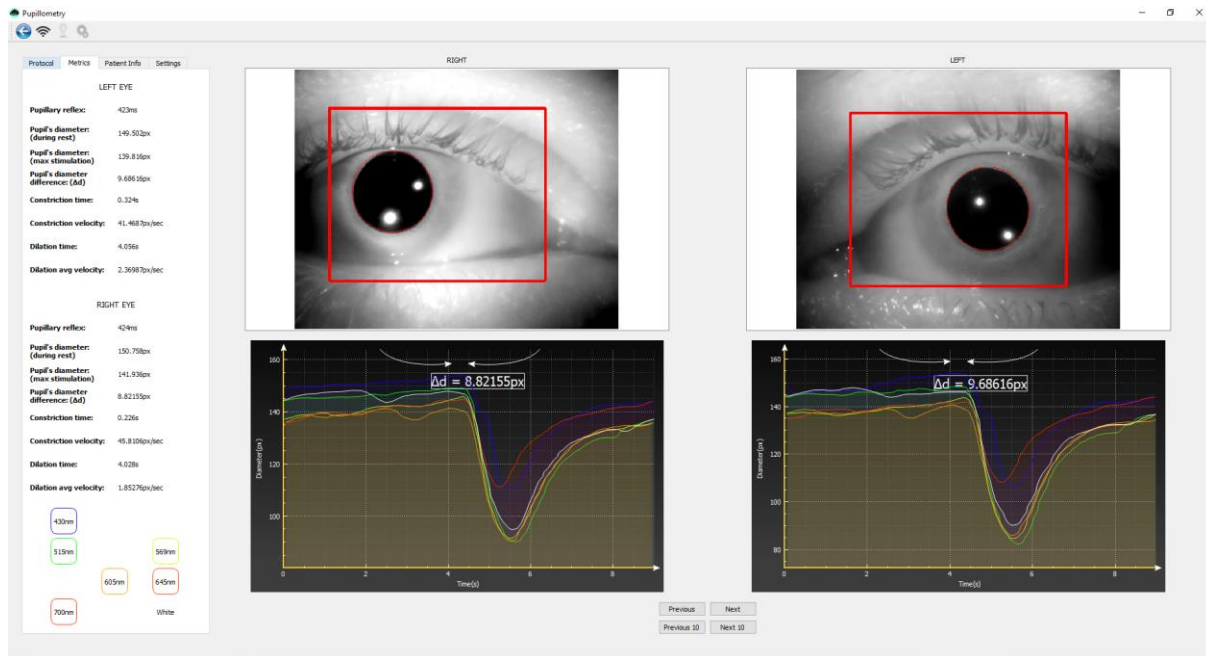


Figure 55: Past Examination Overview

In the left side there is a 4-tab element that contains controls and statistics.

In the top right side the current frame of each eye is visible.

In the bottom right side the graphs <Eye Diameter – Time> are drawn and the four buttons assist us in navigating through the examination's video.

#### 4 Tab Element

The first tab is called “Protocol” and contains information regarding the protocol that was used in the current examination. We can see a) the **name** of the Protocol, b) the duration of the eye's **stimulation** by LED illumination, c) the duration of **resting time** between switching LEDs, d) which eye was triggered (LEFT, RIGHT, BOTH), e) the LEDs used in the order they were used. This tab also contains a “Play Button” that will simulate the examination by playing the video on the top right panels and updating the graph's position on the bottom right.

The second tab is called “Metrics” and contains statistics that the program's backend provides using my own algorithms. In this tab we may also push the colorful buttons to select the graph we want to review. Every button and graph line color corresponds to the color of the stimulus (e.g. Red LED – Red Colors).

The third tab is called “Patient Info” and retrieves data from the “Patient's Profile”, such as age, gender and known conditions (like medical history).

The fourth tab is called “Settings” and is used for debugging and improving the pupil detection parameters.

### Frame Viewers

In the top right section of the page we can see the selected frame of the video (or the whole examination’s video if we choose to). The red rectangle diminishes the region of interest (ROI) for the pupil detection, removing excess noise from shadows caused by eyelashes and the eye’s shape.

The red circle shows my estimation of the pupil. This is technically the pupil detection’s output using image processing. The LEFT, RIGHT labels help us distinguish the two eyes from one another.

### Graphs

The graphs were drawn using the QCustomPlot Library designed for the Qt Platform. The graph is NOT linear, and it resets for each LED. For example if we use the 460nm, 515nm and 730nm LEDs as stimulus, we will have a Blue, a Green and a Red line, each one overlapping the others. This way we can very easily compare the eye’s sensitivity to every color.

The user is able to separate a graph line from the others by clicking on the corresponding wavelength button on the “Metrics” tab.

Every graph line contains some labels. Two of them are the “PLR Start”, “PLR End” labels that show when the LED lighted up and when the eye started reacting to the light. By subtracting  $time(PLR\_END) - time(PLR\_START)$  we can calculate the PLR reflex. The third label is the “ $\Delta$  or Diameter Difference” label.  $\Delta d$  is the subtraction of

$AVG (Diameter (time (RESTING\_PUPIL) )) - Diameter (time (STIMULATED\_PUPIL) )$ ,

where RESTING\_PUPIL contains the frames where the pupil is resting and STIMULATED\_PUPIL contains the frame where the pupil is fully constricted. In other words,  $\Delta d$  is the average resting diameter minus the minimum diameter.



Figure 56: Diameter vs Time, Green Stimulus

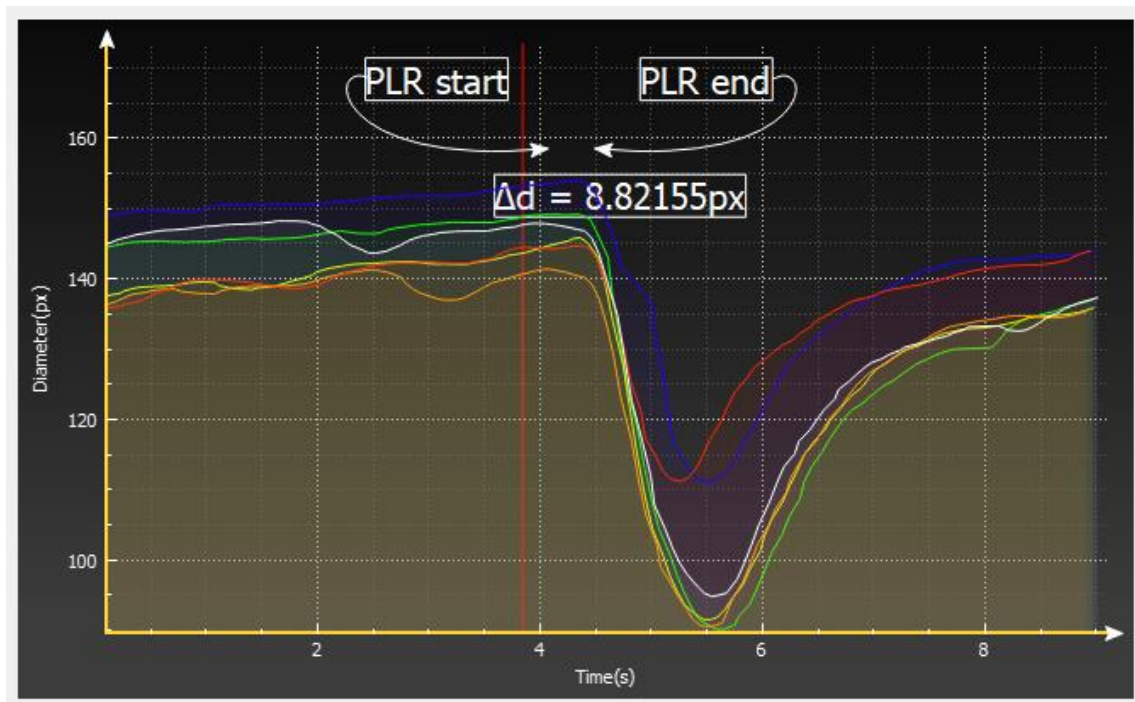


Figure 57: Diameter vs Time, Multiple Stimuli

#### 4.1.4 Recording a new examination (Scanner)

The “Scanner” menu is the page in which all new examinations are recorded and saved. One may choose to simply watch the video feed, commence the threads that measure the pupil, or begin a full examination with certain parameters.

The left side of the page is our control panel. We are able to:

- see the patient’s name
- change all the examination’s parameters to a default preset (e.g. “Red Sensitivity Measurement” protocol will enable Red LEDs and select the appropriate Stimulation and Step times)
- customize the examination’s parameters to a new protocol
- control the video feed and image processing parameters

Examination parameters:

- LED selection
- Stimulation Time: Duration of the stimulus
- Step Time: How long the eye will be resting between stimuli
- R/L Checkboxes: Choose which eye will be stimulated (Right, Left, Both)

Examination process:

1. For *Step\_Time* / 2 seconds, the eye rests.
2. For *Stimulation\_Time* seconds, the eye is stimulated by a chosen LED.
3. For *Step\_Time* / 2 seconds, the eye rests.
4. Repeat steps 1-3 until all the selected stimuli are used.
5. Save all recorded frames into database.

Selecting LEDs:

In order to select multiple stimuli, the user must check the corresponding checkboxes. The LED’s name will then be pushed to the end of a queue. The LED queue is visible on the control panel. By unchecking a LED checkbox, the corresponding LED name will be popped from the queue. The LEDs can be selected in a single click by choosing a default preset. The “Select All” button will push all the LED names into the queue.

X-Ray Button:

As the name suggests, this button provides an outline of the pupil’s contour. This feature is exceptionally useful in helping us understand the way the image processing algorithm detects the pupil. This feature also facilitates debugging the image processing parameters (Thresholds and Area of Interest)

Freeze Image:

This button pauses the video feed.

Infrared (IR):

This bar allows us to control the intensity of the IR illumination LEDs.

“Start Debugging” Button:

This button allows us to monitor the two eyes for an infinite amount of time. The pupil detection threads start working non-stop, until the user clicks “Stop Debugging”. The graphs will record all detected diameters. This feature is particularly helpful, as the user can monitor the eye while it gets accustomed to darkness. When the line drawn is nearly flat, then the pupil is fully accustomed to darkness. The user should then select “Stop Debugging” and click “Start Examination”.

“Start Examination” Button:

This button will commence the examination process as described in the algorithm above.

## 4.2 Backend and Algorithms

This section contains detailed information concerning the algorithms that were created for this project.

### 4.2.1 Image Processing

The human eye pupil’s shape is a slightly imperfect circle. For the purposes of this project, we consider it to be a perfect circle and, thus, use circle detection algorithms.

Two algorithms were created, both equal in efficiency and accuracy. Both will use the parameters: Threshold and Area of Interest.

The images are always gray-scaled before the algorithms process them. The output of this process is an 8-bit Grayscale Image, with intensities from 0-255. Intensity of 0 means the pixel is black, while an intensity of 255 means the pixel is white. To grayscale the image, we choose the camera’s green channel. Most cameras come with an IR-Cut filter, making it impossible to scan near the IR radiation wavelengths. The optimal solution would be to select the wavelengths furthest from the IR-Cut filter; the blue channel, but the green channel is less sensitive to noise and far enough from the cut wavelengths (blue is near 450nm, green is near 550nm, infrared is above 800nm).

The filters and edge detectors are part of the OpenCV library.

#### *First Pupil Detection Algorithm*

Step 1: We scan the image line by line. The first step is finding the max number of serial black pixels.

That is where the pupil should be. This step is particularly fragile in noise from shadows.

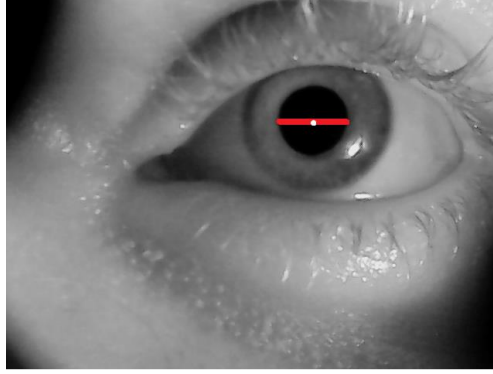


Figure 58: Find max serial black pixels

Step 2: We select the middle pixel of the row in step 1. From the middle pixel we move up until the pixel intensity is higher than the set threshold. We mark that pixel as R1. From the middle pixel we repeat the same process by moving left and then right and mark the new pixels as R2, R3.

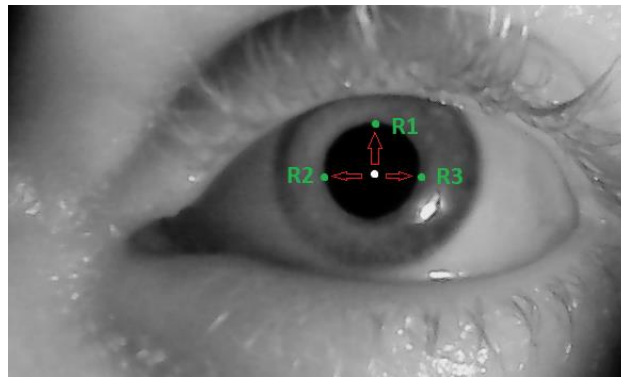


Figure 59: Find three contour points

Step 3: Compute and draw the circle using these 3 points. All we need is the circumcenter and the radius.

The Cartesian coordinates of the circumcenter  $U = (U_x, U_y)$  are

$$U_x = \frac{1}{D} [(A_x^2 + A_y^2)(B_y - C_y) + (B_x^2 + B_y^2)(C_y - A_y) + (C_x^2 + C_y^2)(A_y - B_y)]$$

$$U_y = \frac{1}{D} [(A_x^2 + A_y^2)(C_x - B_x) + (B_x^2 + B_y^2)(A_x - C_x) + (C_x^2 + C_y^2)(B_x - A_x)]$$

The circumradius can be computed as:

$$r = \|U'\| = \sqrt{U_x'^2 + U_y'^2}$$

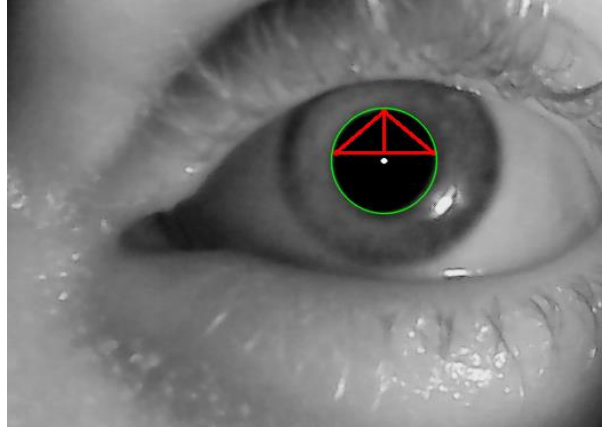


Figure 60: Algorithm's output

### Second Pupil Detection Algorithm

Onto the original image below, the red rectangle represents the Region of Interest (ROI) and the red circle is the final estimation.

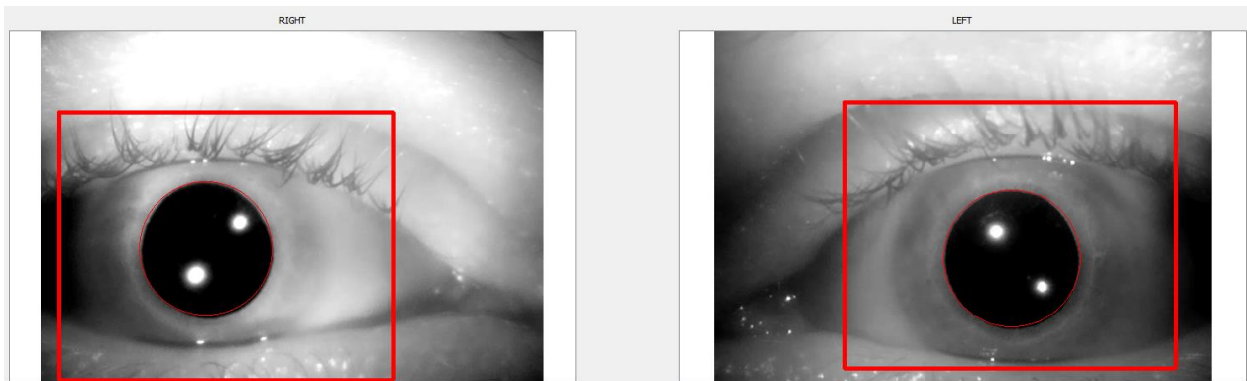


Figure 61: Original Image

Step 1: After the image is gray-scaled, we threshold it using the parameters set by the GUI.

Thresholding means cutting off all intensities over the threshold value. The function we use is:

$$\text{dst}(x, y) = \begin{cases} 0 & \text{if } \text{src}(x, y) > \text{thresh} \\ \text{maxVal} & \text{otherwise} \end{cases}$$



Figure 62: Thresholding the image

Step 2: We use Gaussian blurring with a kernel of  $[3, 3]$ , and standard deviation 2. This step softens the edges.

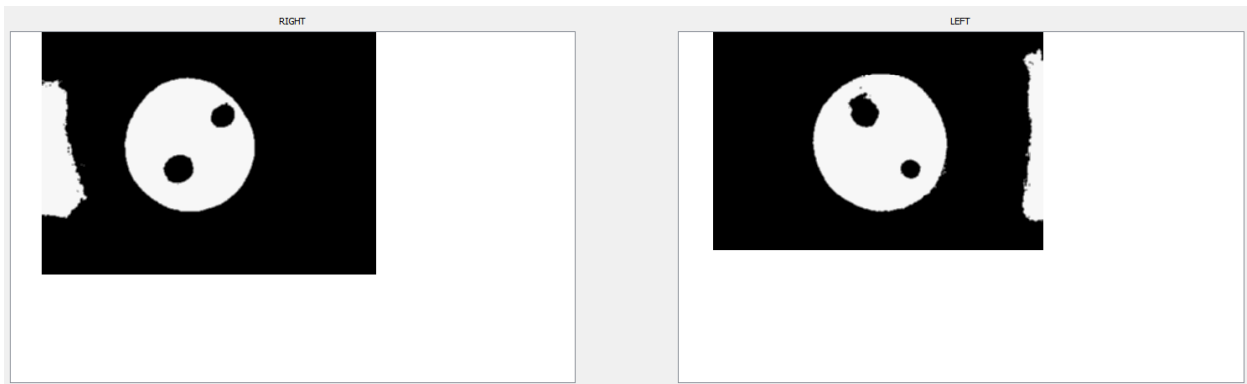


Figure 63: Blurring the thresholded image

Step 3: We will now use a Canny Edge Detector.

The *Canny Edge detector* was developed by John F. Canny in 1986. Also known to many as the *optimal detector*, Canny algorithm aims to satisfy three main criteria:

- **Low error rate:** Meaning a good detection of only existent edges.
- **Good localization:** The distance between edge pixels detected and real edge pixels have to be minimized.
- **Minimal response:** Only one detector response per edge.



Figure 64 : Canny Edge Detector

Step 4: We blur (gaussian blur, kernel of [3, 3], and standard deviation 2) again the image in order to connect and soften the edges. No useful information is lost in this process.



Figure 65: Final output of the image processing

Step 5: We use OpenCV's "findContours" in order to locate all the circle's contours. Using the input parameter "Area of Interest" the tiny spots from the IR LEDs are discarded, and we assess the pupil's diameter correctly.

Step 6: We calculate every single set of contour points until we find a circular set. In order to assess the circularity of a set, we use its area and perimeter.

$$Circularity = 4 * \pi * area / perimeter^2$$

If the result is realistic, (0.2 up to 1.7) then we will keep it as a valid result.

Step 7: We draw and store the results as seen on the "Original Image" in the beginning of "Second Pupil Detection Algorithm".

### 4.2.2 Smoothing and Regression

Detecting the pupil is a very difficult task. Not only is the pupil not a perfect circle, but the image suffers from shadow noise and the eyes are not perfectly still. Due to these reasons, the Diameter vs Image graph may look like this:

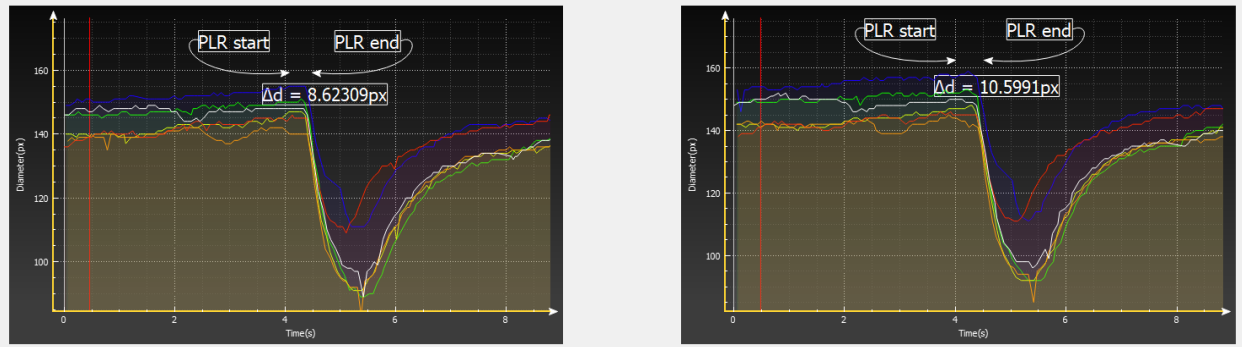


Figure 66: Graphs before smoothing (Left - Right)

These lines are not helpful and may provide us only a very general view of the patient's neurological status. After the smoothing – as seen below – not only do we have a clearer picture of the patient's health, but we can also export useful metrics and statistics within a few milliseconds.

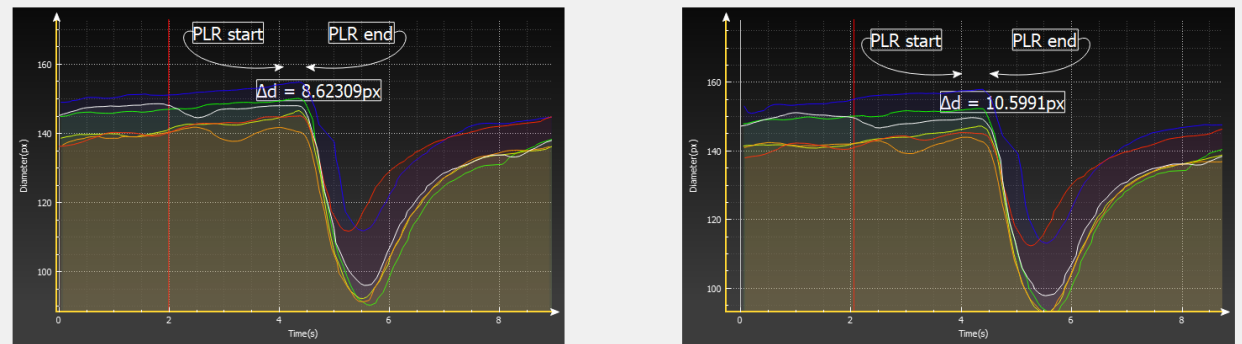


Figure 67: Graphs after smoothing (Left - Right)

In order to achieve this, I have used AlgLib's filtering algorithms.

#### SMA (simple moving average)

Simple moving average filter, denoted as  $SMA(k)$ , is a finite impulse response filter. For any moment  $t$  it returns average of previous  $k$  values (or  $t$  values, for  $t < k$ ). This filter has nice property that for any filter width  $k$  and time series length  $N$  its output can be efficiently calculated in  $O(N)$  time (no dependence on  $k$ ).

### EMA (exponential moving average)

Exponential moving average filter, denoted as  $EMA(k)$ , is an infinite impulse response filter, a transformation of time series according to the formula below:

$$EMA(t) = a \cdot X(t) + (1-a) \cdot EMA(t-1)$$

### 4.2.3 Outlier Detection

Sometimes the examinee's eyes must blink. This is a normal, unavoidable biological process, aimed at preserving the eye's humidity. In this project this phenomenon is very harmful, as the filtering methods described above will take the spikes generated by blinking into account.

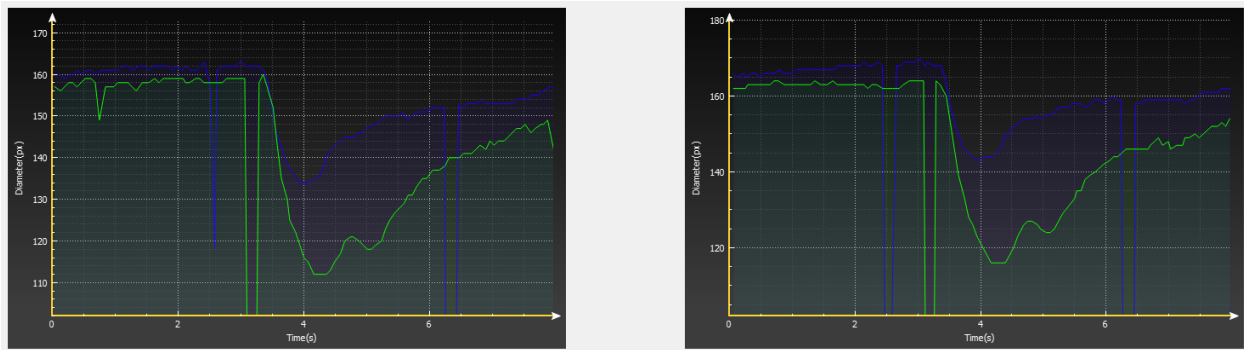


Figure 68: Blinking spikes

My outlier detection algorithm works like this:

Step 1: Locate a frame where the eye has blinked. (Outlier)

Step 2: If  $D(t)$  is the diameter,  $t = \text{time}$ , then I start moving from the outlier towards the left of the graph. If

$$\frac{|D(t-1) - D(t)|}{\max\{D(t), D(t-1)\}} < 15\%,$$

then I have found all of the left neighboring blink frames. The above formula actually evaluates whether the graph line is steep or flat. If the line is relatively flat (15% difference between neighboring frames), then the blinking has stopped. Keep in mind that a blinking eye may be half open, which is even more harmful to the process. That is why the equation above had to be formulated.

Step 3: Repeat step 2 towards the right side, this time the limit being:

$$\frac{|D(t+1) - D(t)|}{\max\{D(t), D(t+1)\}} < 15\%,$$

Step 4: Find the average between the very last frame right before the blink and the very first after the blink stopped.

Step 5: Replace all the blinking frames with the average value.

Below we can see the final result after the filtering; we can observe that the filtering process is completely unaffected!

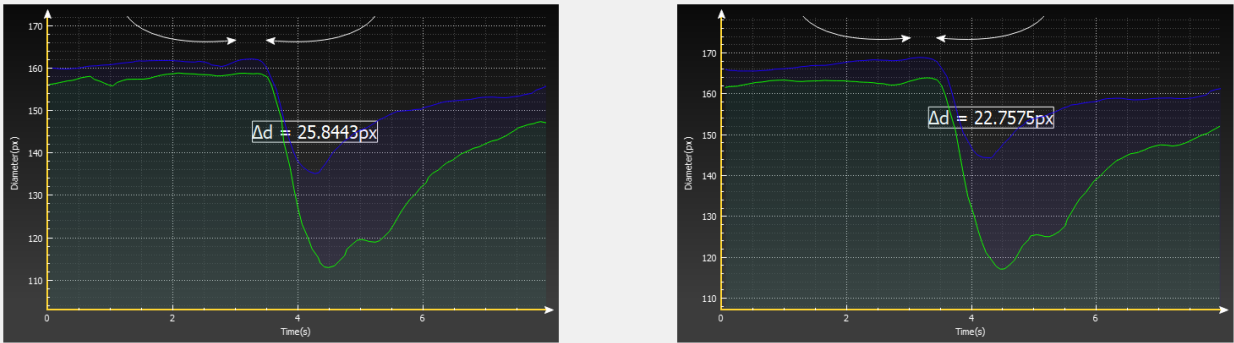


Figure 69: Outlier Detection

#### 4.2.4 Metrics Calculation

The screenshot shows a software interface with four tabs: Protocol, Metrics, Patient Info, and Settings. The Metrics tab is active, displaying data for the LEFT EYE and RIGHT EYE. Below the metrics is a grid of 12 light stimuli buttons, each with a wavelength value.

LEFT EYE	
<b>Pupillary reflex:</b>	235ms
<b>Pupil's diameter: (during rest)</b>	141.489px
<b>Pupil's diameter: (max stimulation)</b>	107.964px
<b>Pupil's diameter difference: (<math>\Delta d</math>)</b>	33.5244px
<b>Constriction time:</b>	0.714s
<b>Constriction velocity:</b>	49.6916px/sec
<b>Dilation time:</b>	2.132s
<b>Dilation avg velocity:</b>	13.0362px/sec

RIGHT EYE	
<b>Pupillary reflex:</b>	129ms
<b>Pupil's diameter: (during rest)</b>	139.157px
<b>Pupil's diameter: (max stimulation)</b>	106.741px
<b>Pupil's diameter difference: (<math>\Delta d</math>)</b>	32.4163px
<b>Constriction time:</b>	0.806s
<b>Constriction velocity:</b>	42.857px/sec
<b>Dilation time:</b>	2.191s
<b>Dilation avg velocity:</b>	12.4794px/sec

430nm	460nm	515nm
535nm	569nm	569nm
587nm	605nm	645nm
700nm	730nm	White

A Diameter vs Time graph is not really useful unless computer generated statistics and metrics are calculated and displayed.

This is why this GUI element was fabricated. It contains all information about the eye's performance under each stimulus.

The user may very easily switch between the different stimuli using the colorful buttons.

- **Pupillary Reflex:** The approximate time between the LED turning ON and the eye reacting to it. This is essentially the Pupillary Light Reflex (PLR).
- **Pupil's Diameter:** The diameter during rest is an average from the beginning until the moment the LED turns ON. The diameter during stimulus is the minimum diameter calculated during the stimulus. The difference between these two is also calculated and printed both in the table and inside the chart area.
- **Constriction Time and Velocity:** The time required until the pupil is fully constricted, and the steepness of the  $D(t)$  function during the stimulation.
- **Dilation Time and Velocity:** The time required until the pupil is fully dilated, and the **average** steepness of the  $D(t)$  function during the dilation.

These processes are resolved by:

1. Selecting a starting point (e.g. when the LED turns ON).
2. Moving towards the right until reaching an *empirical* threshold (e.g. the 63% of the original value)
3. Averaging and mathematically calculating the results.

All of these processes are over in a total of few milliseconds.

## 4.2.5 Technical Information

### *Multithreading*

Multithreading is essential, as this project requires heavy tasks being executed simultaneously, without blocking the UI processes.

My program takes full advantage of Windows' Multi-Threading, implemented by Qt as QThreads.

The threads used are:

- UI thread (Master Thread), responsible for the Graphics User Interface and many lightweight operations, affecting the UI.
- Pupil Measurement (Worker Thread), responsible for calculating the pupil's diameter **live**, without blocking the UI.
- Video Decoding (Worker Thread), responsible for decoding the received frames to readable data.
- Offline Video Playback (Worker Thread), responsible for playing back video and updating the UI when reviewing examinations.

### *Device – Computer Connection*

In order to connect the two devices, our software team generated a “Server” program and installed it inside the Raspberry Pi s. We use Putty to connect to the device via SSH and then start the server program in both Raspberries. After that, a connection can be formed through TCP channels, streaming continuously data of approx. 15Mbps. This program was generated in Qt platform, using C++.

### *Raspberry Video Encoding*

The Raspberries encode the raw video feed into H.264 using the MMAL (Multimedia Abstraction Layer) library. After updating the Raspberries' firmware, the MMAL library was compiled and installed via Putty (SSH).

#### 4.2.6 Database

For the purposes of this project, an SQLite Database was the optimal solution, since SQLite is:

- Fully portable - needs no extra installations or running servers.
- Very fast when there are no simultaneous connections – there are none in this project.
- Fully supported by the Qt Platform.

#### *Table Schema*

- Charts: This table will be used in later versions to aid in machine learning. Whenever we save an examination of satisfying quality, all the metric data are stored here.
- Conditions: Contains all of the “known conditions”.
- Conditions of patients: Associates a condition (e.g. autism) to a patient. This will be really helpful in later versions when machine learning is available.
- Exams: All the info regarding an examination.
- Patients: All the info concerning a patient – examinee.
- Photos: Every single video frame, along with the exam number and timestamp.
- Protocols: Default protocols to speed up the exam process. (A protocol consists of stimulation time, chosen LEDs and resting time)
- Protocols Custom: Associates protocols to examinations.
- Users: All the info regarding the examiner.

The photos are stored in a “BLOB” format. This means that my program will convert every frame to either JPEG or PNG (JPEG is smaller and faster, while PNG has better quality), and then to binary data. The binary data will be stored in a row as “BLOB” inside the “photos” table.

## 4.2.7 Flowchart

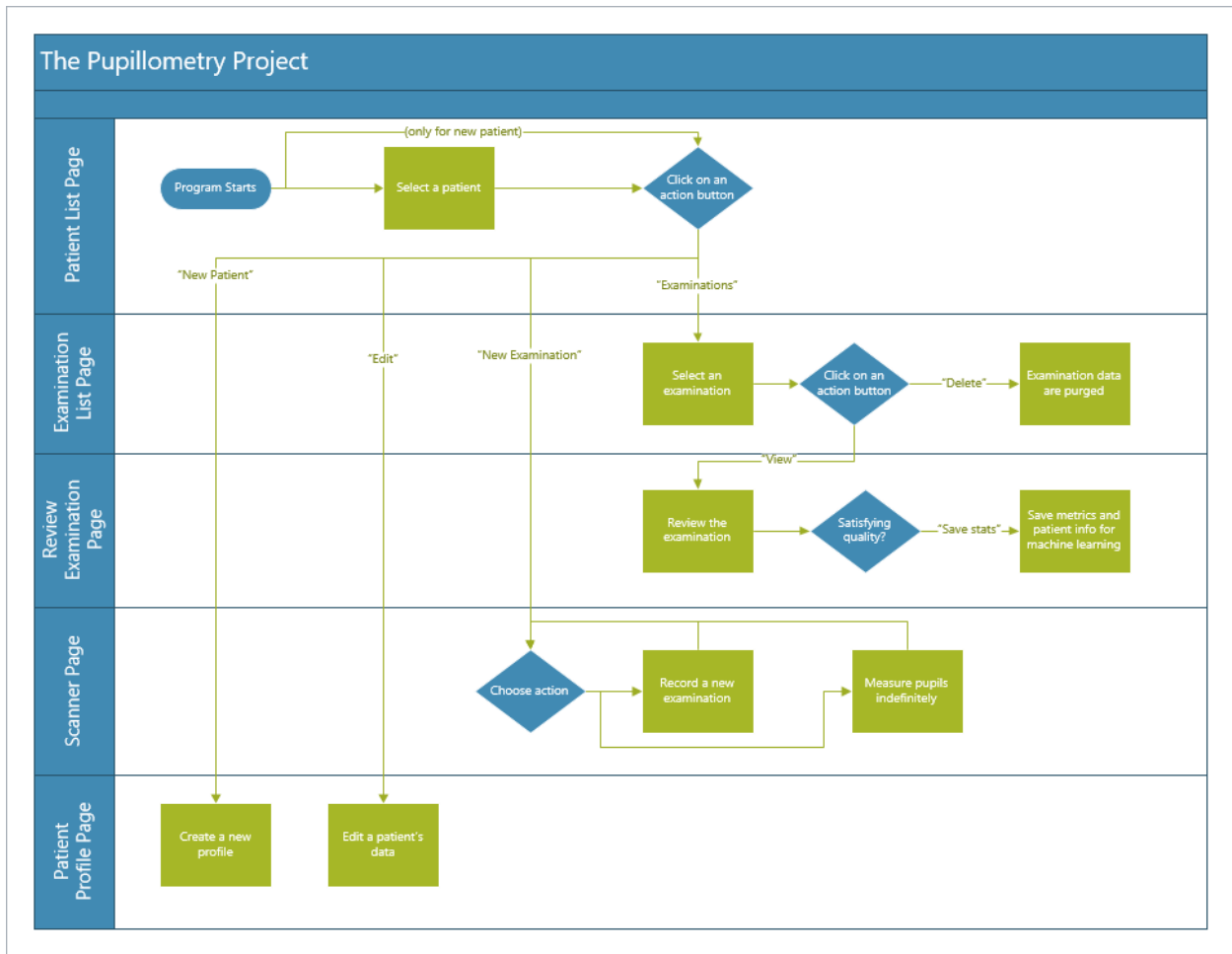


Figure 70: Graphical User Interface Flowchart

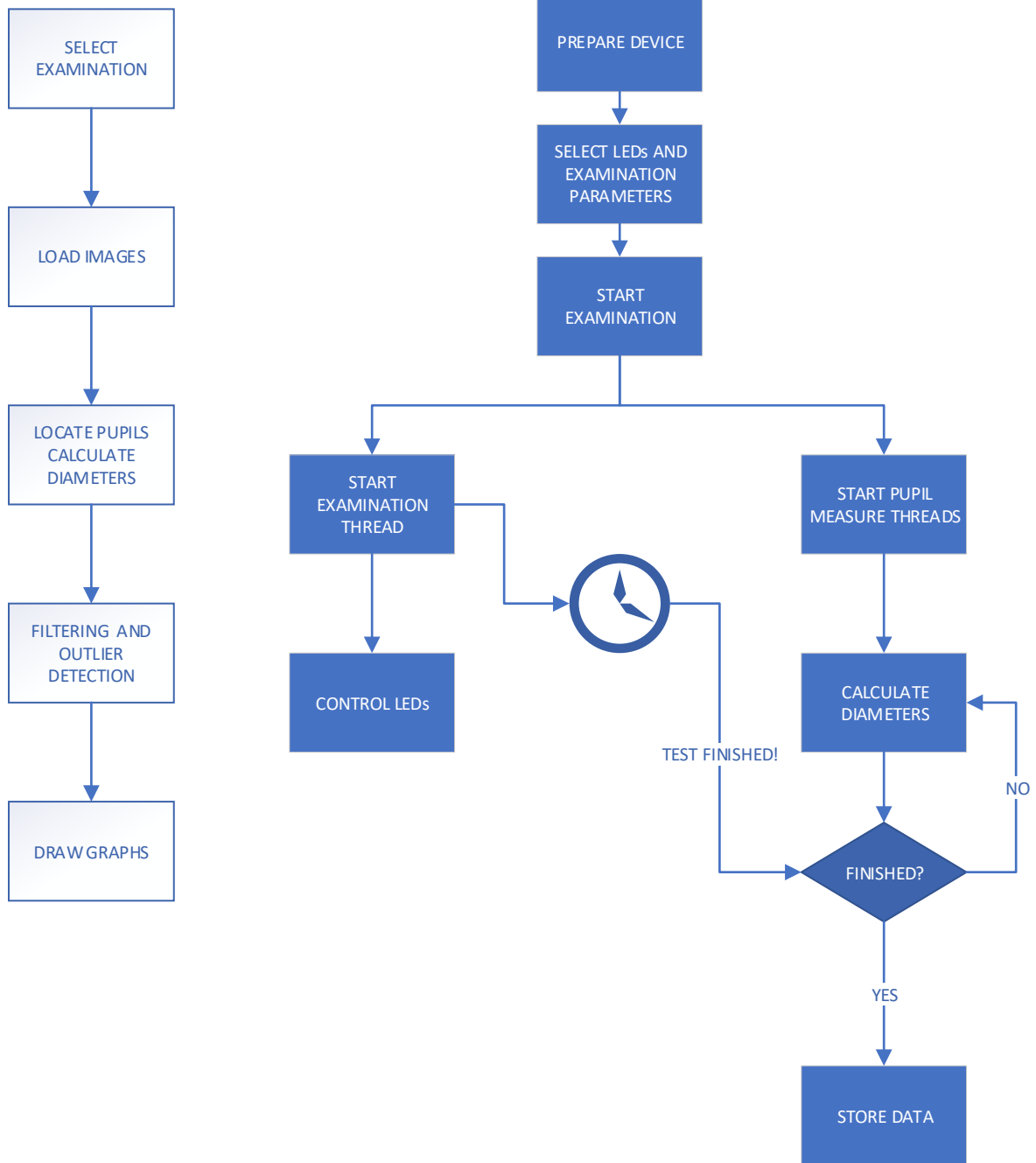


Figure 71: Software Flowchart

## Part 5: Measurements and results

All results are computer generated (see 4.2.4). More highly detailed metrics will be added in a later version of the program. All examinations may be reviewed in the “Review Examination” page.

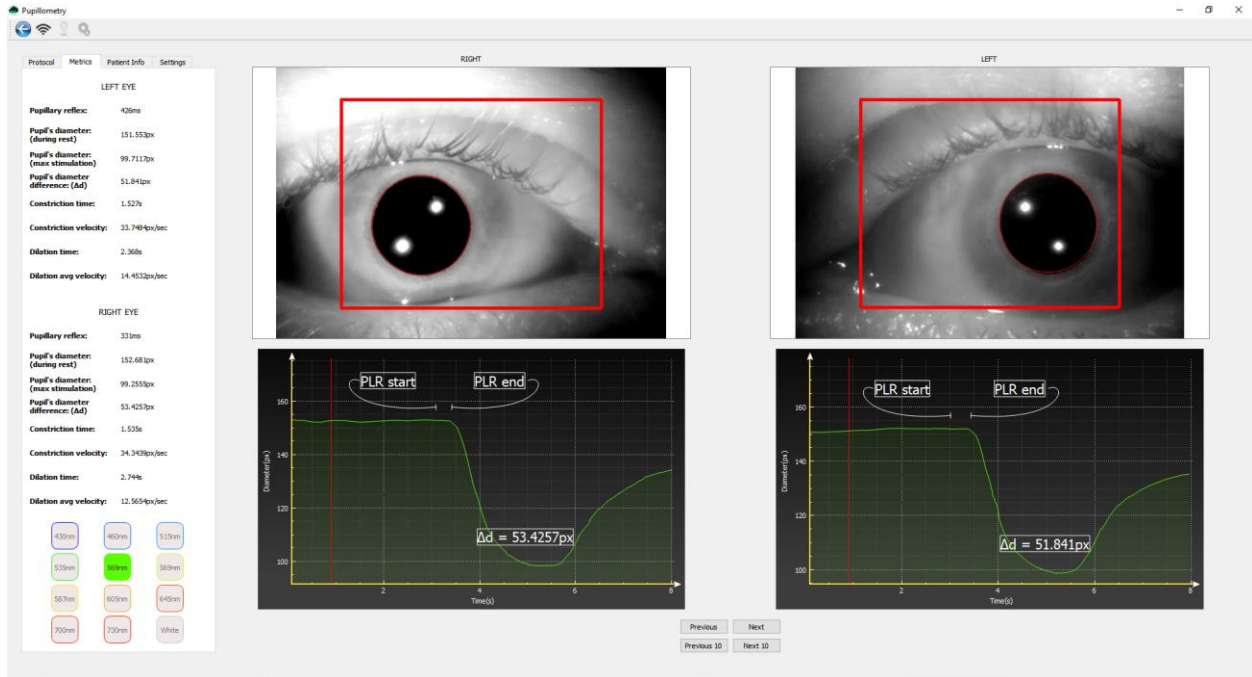


Figure 72: Reviewing Examinations

Key points for a high quality examination:

- No spikes and other harmful fluctuations with no clinical significance.
- The curves must be smooth, without “waves” or “thorns”.
- The expected pattern of the line’s path must be visible, meaning that all examinations should look *similar* to the above.

Proper pattern key points:

- Before the first LED stimulus, the line must be as flat as possible. During an examination that contains multiple stimuli, the eye may have not fully recovered if the resting time is not long enough.
- During the stimulation, a small portion in the beginning will be still flat, as the eye rarely reacts faster than 300ms. After the stimulation, the same pattern is visible, with a slightly increased duration.
- During the dilation, the eye quickly reaches the 63% barrier and then recovers really slowly. While the eye tries to accommodate to the darkness, the graph may appear sinusoid (wavy), as the eye keeps making micro-changes in order to re-accommodate to darkness.

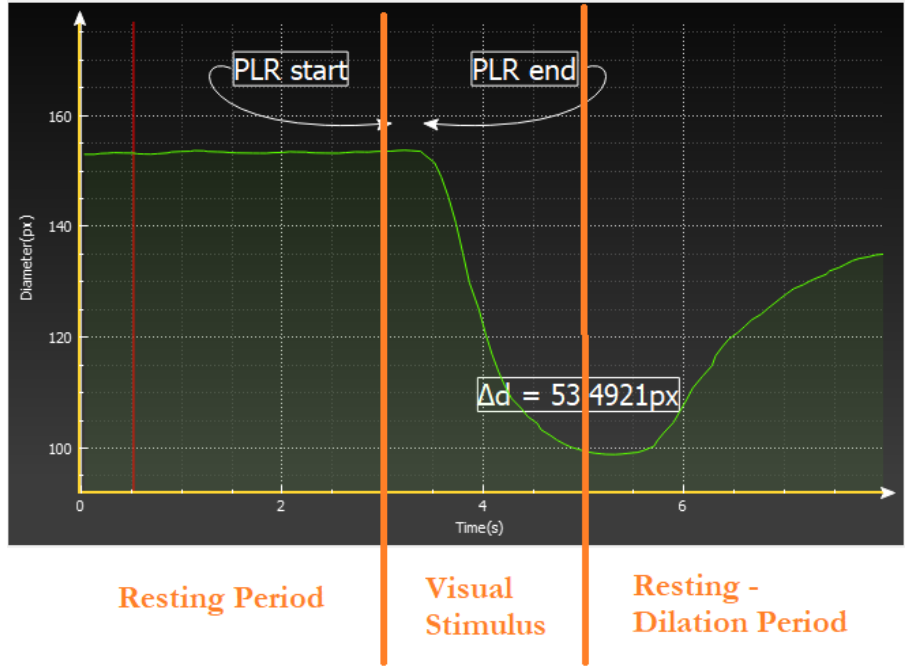


Figure 73: Examination patterns

### 5.1 Eye's adaptability

An interesting remark is that the eye may not get adapted to the visual stimulation instantaneously. Instead, the eye's diameter will overshoot way below the needed diameter and the eye will respond once more to the new brightness, dilating until the brightness is comfortable and safe for the retina.



Figure 74: Slow accommodation to light

This is a normal process, concerning homeostasis. By measuring the speed of the eye's adaptability and the diameter difference between high and low points, we may be able to provide a metric regarding the speed and quality of the examinee's homeostatic control. This process *may* allow us to detect homeostatic imbalances.

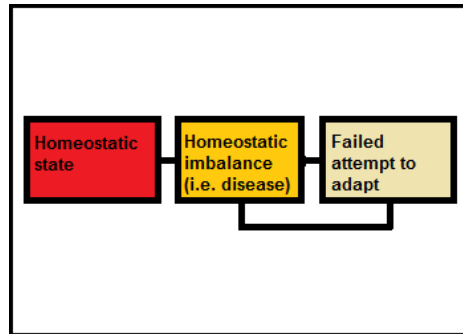


Figure 75: Homeostatic imbalance

## 5.2 Multicolor stimulation

During the development of this project I have developed three different ways of presenting the graphs:

- Linear: The line starts from 0 and stops when the examination is over.
- Multicolor Overlapping:
  - There are 3 phases: Resting, Stimulation, Resting.
  - For each LED color we will execute these three phases and print them exactly as it happened.
  - For each new LED we reset the time to 0.
- Multicolor Overlapping Extended:
  - There are 3 phases like in Multicolor Overlapping.
  - The last phase is extended by copying the next LED's first phase.



Figure 76: Graph drawing timelines

Multicolor Overlapping Extended clearly gives us a clearer picture of the eye's reactivity to different color stimuli; see figures below:

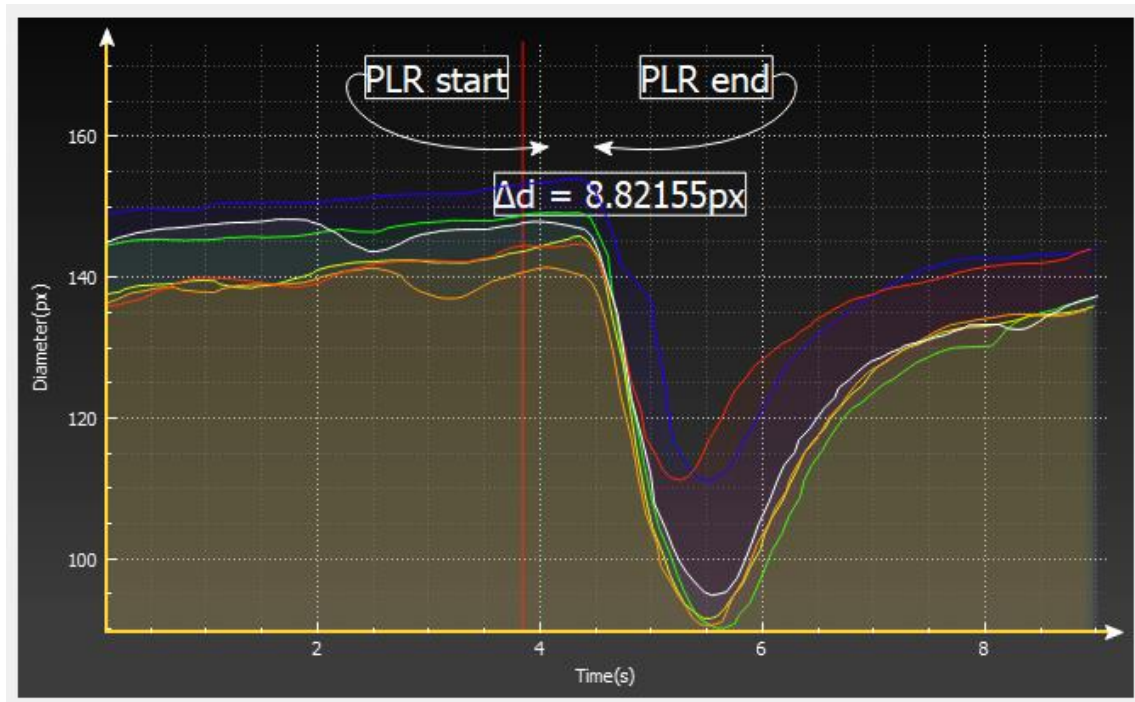


Figure 77: Multicolor Overlapping

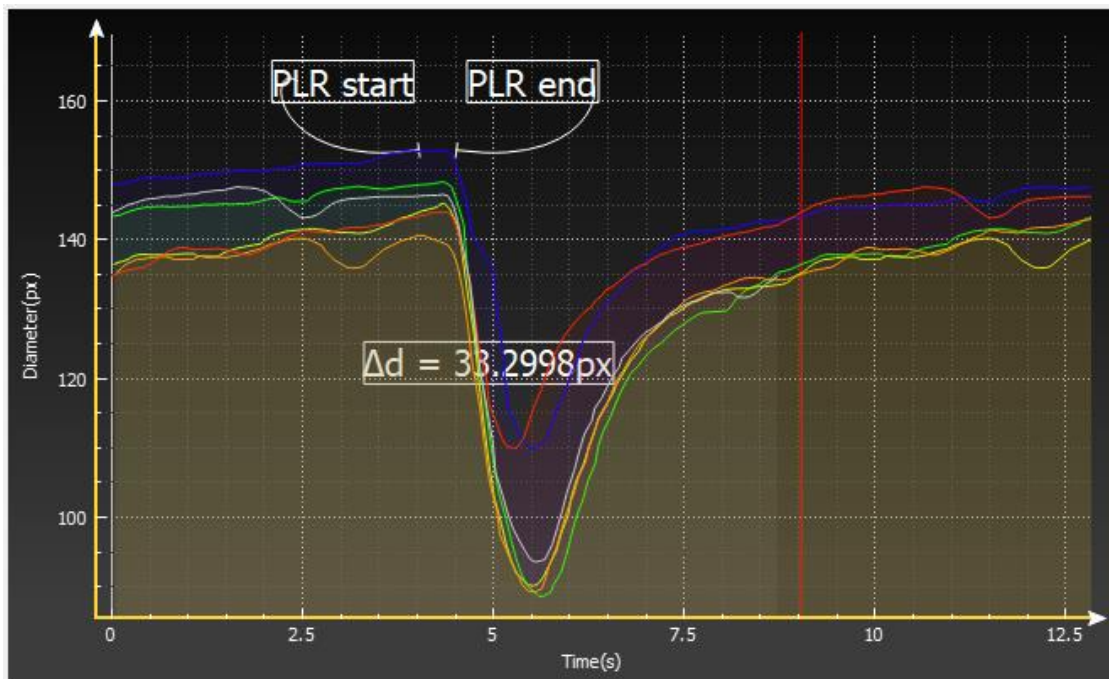


Figure 78: Multicolor Overlapping Extended

## References

[1] Physics of the Human Eye

Charlie Chen, Kevin Sun, Alborz Kia, Vince Milczek, Alan An

McGill University Department of Physics

Source: <http://www.physics.mcgill.ca/~hilke/181/projects/PHYS181%20Project%20-%20Physics%20of%20the%20Human%20Eye.pdf>

[2] A short review and primer on pupillometry in human computer interaction applications

Oswald Barral

[3] Chromatic Pupillometry in Children

Sylvain V. Crippa, Fatima Pedrosa Domellöf and Aki Kawasaki

[4] Tracking the Dynamics of Mind Wandering: Insights from Pupillometry

Claudia Pelagatti, Paola Binda and Manila Vannucci

[5] Pupillometry in Infancy Research

Robert Hepach & Gert Westermann

[6] Pupillometric Assessment of Sleepiness in Narcolepsy

Bharati Prasad, Young K. Choi, Terri E. Weaver and David W. Carley

[7] Utility of dynamic pupillometry in alcohol testing on drivers

Luis Lucio Lobato-Rincón, María Carmen Cabanillas Campos, Juan José Navarro-Valls, Cristina Bonnin-Arias, Eva Chamorro. Celia Sánchez-Ramos Roda

[8] Pupillary Light Reflex is Altered in Adolescent Depression

A. MESTANIKOVA, I. ONDREJKA , M. MESTANIK, D. CESNEKOVA, Z. VISNOVCOVA, I. BUJNAKOVA, M. OPPA , A. CALKOVSKA, I. TONHAJZEROVA

[9] Source: Wikipedia. Topics: Human Eye, Optic Nerve, Oculomotor Nerve, Sympathetic and Parasympathetic Nervous System, Autonomic Nervous System, Pupillary Light Reflex, H.264.

[10] <https://www.raspberrypi.org>

<https://www.arduino.cc>

Datasheets from: [www.mouser.com](http://www.mouser.com)

[11] Dose-Dependent Effects of Androgens on the Circadian Timing System and Its Response to Light

April 2012 Endocrinology 153(5):2344-52

DOI: 10.1210/en.2011-1842 PubMed

Matthew P Butler, Ilia N Karatsoreos, Joseph Lesauter, Rae Silver

[12] Homeostatic Imbalance: Definition & Examples

<https://study.com/academy/lesson/homeostatic-imbalance-definition-examples.html>

[13] Eye Safety for Proximity Sensing Using Infrared Light-emitting Diodes

<https://www.intersil.com/content/dam/Intersil/documents/an17/an1737.pdf>